Source-To-Sink Sedimentary Budget of the African Equatorial Atlantic Rifted Margin

Delphine Rouby, Jing Ye, Dominique Chardon, Artiom Loparev, Mark Wildman, Massimo Dall'Asta

Geochemistry, Geophysics, Geosystems®

AGU ADVANCING EARTH AND SPACE SCIENCES

RESEARCH ARTICLE
10.1029/2023GC010901

Source-To-Sink Sedimentary Budget of the African Equatorial Atlantic Rifted Margin

Delphine Rouby[1], Jing Ye[1,2], Dominique Chardon[1], Artiom Loparev[1], Mark Wildman[3], and Massimo Dall'Asta[4]

[1]Géosciences Environnement Toulouse, Université de Toulouse, CNRS, IRD, UPS, CNES, Toulouse, France, [2]Ali I. Al-Naimi Petroleum Engineering Research Center, King Abdullah University of Science & Technology, Thuwal, Saudi Arabia, [3]School of Geographical and Earth Sciences, College of Science and Engineering, University of Glasgow, Glasgow, UK, [4]TotalEnergies, Centre Scientifique et Technique Jean Féger, Pau, France

Key Points:

- The sub-saharan West Africa cratonic domain underwent only very low steady denudation rates (<10 km/Ma) since Equatorial Atlantic rifting
- Equatorial Atlantic rifting altered the cratonic denudation only transiently, in a narrow domain corresponding to rift-related relief erosion
- Post-rift accumulation rates in the rifted margin basins were thus controlled by global climate change and/or drainage reorganizations

Supporting Information:

Supporting Information may be found in the online version of this article.

Correspondence to:

D. Rouby,
delphine.rouby@get.omp.eu

Citation:

Rouby, D., Ye, J., Chardon, D., Loparev, A., Wildman, M., & Dall'Asta, M. (2023). Source-to-sink sedimentary budget of the African Equatorial Atlantic rifted margin. *Geochemistry, Geophysics, Geosystems*, *24*, e2023GC010901. https://doi.org/10.1029/2023GC010901

Received 10 FEB 2023
Accepted 5 SEP 2023

Abstract Despite their very low relief and erosion rates, non-orogenic (i.e., cratonic) continental domains account for over 60% of the Earth's exposed lands. Therefore, they contribute significantly to the clastic sediments and solutes exported to the ocean and should be accounted for in global studies. Nonetheless, they have been much less studied than orogenic domains. In this study, we establish the source-to-sink sedimentary budget of the sub-saharan West African cratonic domain and its Equatorial Atlantic rifted margin using published low-temperature thermochronological data to estimate onshore denudation and regional geological cross-sections to estimate offshore accumulation. We show that during and immediately following rifting (130-94 Ma), the build-up and subsequent erosion of rift-related relief resulted in a transient, 100–200 km wide strip along the margin recording high denudation rates (>50 m/Myr), while the inland domain underwent steady and very low denudation (<10 m/Myr). Afterward, the whole onshore domain underwent very low and steady denudation. Thus, the changes in post-rift accumulation rates documented along the rifted margin were caused by changes in the climate and/or drainage network. During the Late Cretaceous, we document a regional rise in accumulation rates caused by the enlargement of drainage areas feeding the basins by a hinterlandward migration of the continental divide. During the Paleogene, we document a general drop in accumulation rates in all the basins of the African Atlantic margins caused by the global greenhouse climate, which enhanced the development of lateritic weathering mantles, storing clastic sediments on the continent and favoring solute exports to the ocean.

Plain Language Summary Cratons, shields and continental platforms have low relief and erode very slowly. As a result, they are often neglected while investigating sediment routing systems at the surface of the Earth over geological times. In this study, we determine the source-to-sink sedimentary budget of the sub-saharan part of West Africa and its equatorial Atlantic margin. To do this, we estimate the histories of (a) erosion on the continent and (b) accumulation in the offshore basins. We show that the sub-saharan region of West Africa has experienced very little erosion since at least 200 Ma. The only exception was the temporary removal of relief caused by the rift that split Africa and South America. Following that rifting, variations in sediment accumulation in the basins were driven by changes in climate that modified the way the continent was being eroded or by modifications of the river courses carrying sediments to the ocean.

1. Introduction

The contribution of non-orogenic continental domains (i.e., platforms, cratons and shields) to global sediment export to the oceans is often overlooked because their relief and erosion rates are very low (typically <10 m/Myr; Beauvais and Chardon (2013)). Nevertheless, the vast dimensions of non-orogenic domains (which cover over 60% of continental surfaces) allow them to currently contribute up to 30%–40% of the clastic sediments exported by continents to the global ocean (Maffre et al., 2018; Milliman & Farnsworth, 2011). Sediment routing systems transport sediments from production areas, across domains of transit and/or transient storage, to their ultimate sedimentary basins. The goal of "Source-to-Sink" studies is to better understand the dynamics of these systems by quantifying continental erosion, sediment fluxes and terminal basin accumulations (e.g., Allen, 2008; Bhattacharya et al., 2016; Grimaud et al., 2018; Rouby et al., 2009; Schumm, 1981; Sømme et al., 2009). Indeed, variations in continental erosion and accumulation rates in sedimentary basins may reveal tectonic events, climate changes or drainage reorganizations in the source area that affect sediment production, availability and

transport to the sedimentary basins. However, most of the studied sediment routing systems are those of orogenic domains, characterized by rapid and high-magnitude rock uplift as well as high sediment fluxes (e.g., Allen et al., 2013; Kuhlemann et al., 2002; Wittmann et al., 2016; Zattin et al., 2014). Only a few studies have attempted to quantify sediment exports in non-orogenic/cratonic domains (Baby et al., 2020; Charton et al., 2020; Grimaud et al., 2018; Pazzaglia & Brandon, 1996; Poag & Sevon, 1989; Rouby et al., 2009; Rust & Summerfield, 1990; Tinker et al., 2008). Yet, the sediment routing systems of cratonic domains are expected to be very different from those of orogenic domains because of the slow and low vertical movements (i.e., epeirogeny) that typify shields.

Sub-saharan West Africa (here defined between 20°N, 5°E and the Atlantic Ocean rifted margin in the west and south; Figure 1) is one of the best documented non-orogenic continental domains over geological timescales. Indeed, Beauvais and Chardon (2013), Chardon et al. (2016), and Grimaud et al. (2018) used the spatial distribution of dated relict Cenozoic lateritic paleo-landforms to assess its relief evolution and quantify its erosion. These studies have identified an upward domain along the margin ("marginal upwarp") that focused up to 10–12 m/Myr of denudation since 45 Ma, while the rest of the region had undergone less than 4 m/Myr of denudation over the same period. Chardon et al. (2016) also showed that the topographic growth of the Hoggar hotspot swell (north of the Iullemmeden Basin; Figure 1) triggered a large-scale drainage re-organization at ca. 34 Ma that increased the size of coastal catchments, which correlates with higher accumulation rates in the basins of the Equatorial Atlantic rifted margins and initiation and growth of the modern Niger river delta (Grimaud et al., 2018). In contrast, the very low Paleocene-Eocene (65–34 Ma) accumulation rates in the rifted margin basins (Grimaud et al., 2018) were attributed to greenhouse climate-induced chemical weathering of the continental domain that favored sediment storage as lateritic regolith in weathering profiles and exports of solutes produced by chemical weathering (see Chardon, 2023). Ye et al. (2017) showed that, between the onset of rifting in the Early Cretaceous and 45 Ma, the primary source for sediments routed to the rifted margins was the Leo-Man shield and its fringing Proterozoic and Paleozoic platform sedimentary cover (Figure 1). However, the relief, drainage configuration and erosion dynamics of the region before 45 Ma remain to be deciphered.

In this contribution, we address the cratonic sediment routing systems by investigating sub-saharan West Africa and its Equatorial Atlantic rifted margin (Figure 1) since the onset of rifting ca. 140 Ma ago (e.g., Basile et al., 2005). We build upon previous studies that documented and constrained (a) its evolving Mesozoic to Cenozoic paleogeographic and structural framework (Ye et al., 2017), (b) its Cenozoic erosion history (Beauvais & Chardon, 2013; Grimaud et al., 2018), (c) the thermal history of its onshore portion (e.g., Wildman et al., 2018, 2022 and references therein) and (d) the crustal and stratigraphic architecture of its Equatorial rifted margin (e.g., Bennett & Rusk, 2002; Brownfield & Charpentier, 2006; Ye et al., 2019).

Most of the source-to-sink studies usually concentrate on quantifying either the continent denudation or the sedimentary basin accumulation. In this study, we adopt a novel quantitative source-to-sink approach to establish the very long-term budget of both denudation and accumulation of a wide cratonic domain and its fringing rifted margin in order to investigate the respective contributions of tectonics (i.e., rifting), drainage reorganization or climate (i.e., greenhouse/icehouse) to its continental relief evolution and the accumulation histories of the rifted margin. We use published low-temperature thermochronological data to estimate onshore denudation patterns and build geological regional cross-sections to estimate offshore accumulation histories of the rifted margin basins (from Sierra Leone to Benin).

2. Geological Outline and Earlier Works

The African Equatorial Atlantic rifted margin is separated from the Central Atlantic rifted margin by the Guinea Fracture Zone and from the South Atlantic rifted margin by the Chain Fracture Zone (Figure 1a). It is composed of three segments and their associated basins: the Sierra Leone-Liberia, Ivory Coast-Ghana, and Togo-Benin Basins. The segments are separated by the Saint Paul and Romanche Fracture Zones. Rifting of the Equatorial Atlantic was initiated in the earliest Cretaceous (ca. 145–130 Ma) (e.g., Figueiredo et al., 2007; Gouyet, 1988). During the Aptian (ca. 120–115 Ma), an en-échelon strike-slip rift system developed (e.g., Basile et al., 2005; Ye et al., 2017), forming large pull-apart basins that preserved thick continental to shallow-marine sediments (e.g., Antobreh et al., 2009; Bennett & Rusk, 2002; Brownfield & Charpentier, 2006) (Figure 1b). Rifting eventually led to the continental break-up, and the end of crustal extensional deformation is marked by a Late Albian regional break-up unconformity (ca. 104 Ma) on both the African and South American conjugate rifted margins (e.g., Antobreh et al., 2009; Bennett & Rusk, 2002; Brownfield & Charpentier, 2006; Figueiredo et al., 2007;

10.1029/2023GC010901

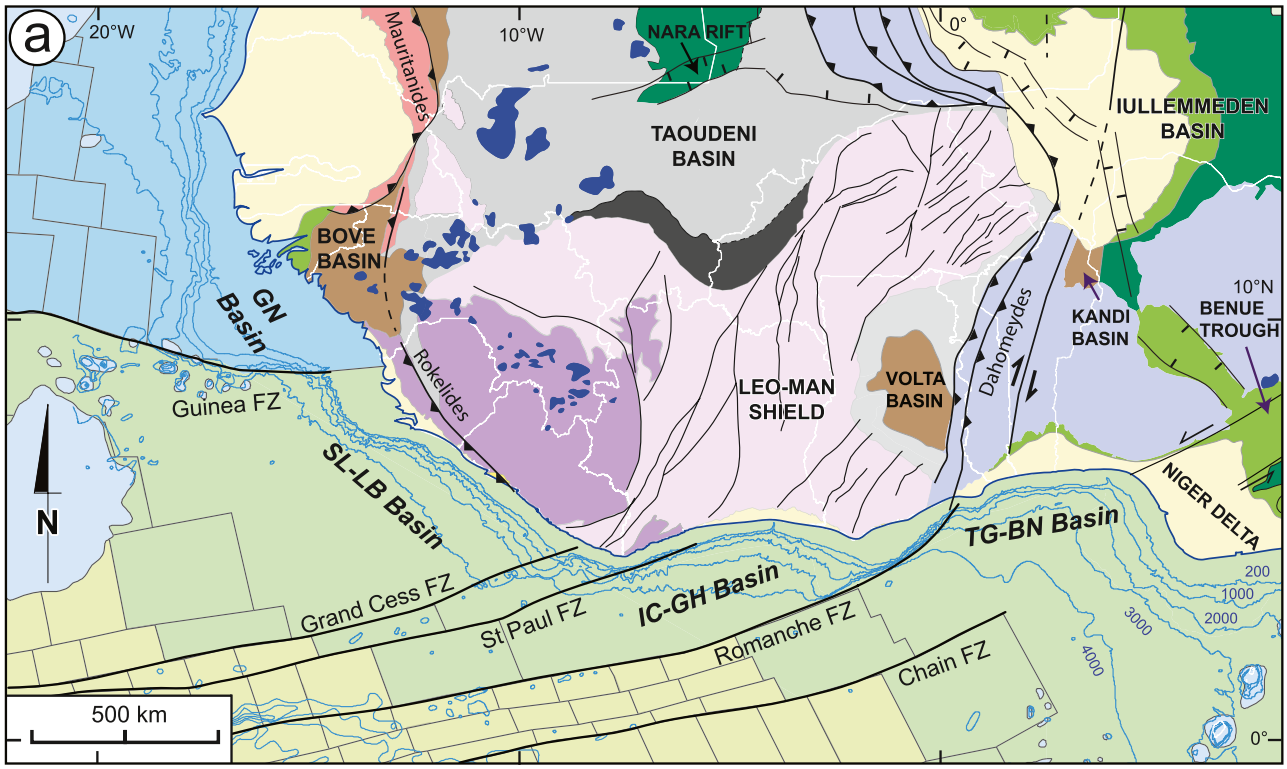

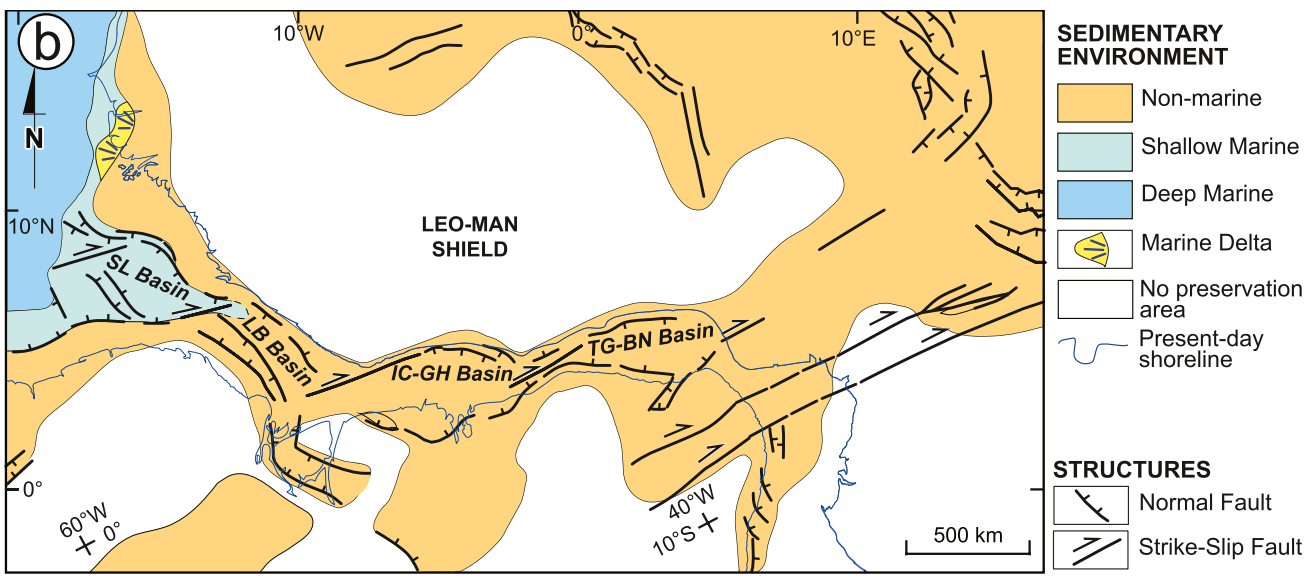

Figure 1. (a) Geological map of the study area. Archean and Paleoproterozoic terrains of the Leo-Man shield constitute the main outcrops of sub-saharan West Africa. Blue lines are present-day bathymetric contours (labeled in meter). International borders are shown by white lines. Compiled after Choubert and Faure-Muret (1988), Deynoux et al. (2006), Milesi et al. (2010), Couëffé and Vecoli (2011), and Ye et al. (2017). (b) Simplified Aptian (120–115 Ma) paleogeological map of the study area (fixed Africa) showing deposition area and environments (modified after Ye et al. (2017)). GN: Guinea; SL-LB: Sierra Leone-Liberia; IC-GH: Ivory Coast-Ghana; TG-BN: Togo-Benin; FZ: Fracture Zone.

Ye et al., 2019). The Central and South Atlantic Oceans then connected through initially isolated "oceanic crust basin" patches (e.g., Blarez & Mascle, 1988; Ye et al., 2017). In the Late Albian, the African Equatorial rifted margin had acquired its segmentation with alternating transform and divergent segments formed along former strike-slip and normal faults, respectively (e.g., Markwick et al., 2021; Ye et al., 2019) (Figure 1). After the continental break-up, the tectono-stratigraphic evolution of the rifted margin was predominantly driven by thermal subsidence, allowing for the preservation of thick Upper Cretaceous-Cenozoic siliciclastic deposits including limited amounts of carbonates (e.g., Bennett & Rusk, 2002; Brownfield & Charpentier, 2006; Ye et al., 2019).

The Archean-Paleoproterozoic Leo-Man shield is the main crystalline outcrop of West Africa, forming the basement of the hinterland of the rifted margin. The shield is flanked by the Rokelides and Mauritanides mobile belts to the West and the Dahomeides orogen and its Volta foreland basin to the East (Figure 1a). The Leo-Man shield supports the Mesoproterozoic-Mesozoic Taoudeni Basin and is fringed to the NE by the Paleozoic-Cenozoic Iullemmeden Basin. Both basins preserve Lower Cretaceous non-marine sediments known as the "Continental Intercalaire" (e.g., Dars, 1957; Kilian, 1931; Lefranc, 1983; Lefranc & Guiraud, 1990). The Precambrian and Phanerozoic platform cover of West Africa is made almost exclusively of sandstones and siltstones, whereas basement rocks are mostly granitoids, with some proportions of volcano-sedimentary rocks found in greenstone belts of the Leo-Man shield.

The present-day drainage of West Africa stabilized at around 30 Ma (Chardon et al., 2016). It may be divided into four main drainage systems: (a) the Short Atlantic drainages along the Guinean and Sierra Leone—Liberia rifted margins, (b) the Long Atlantic drainages along the Ivory Coast-Ghana and Togo-Benin rifted margins, (c) the Senegambia catchment, to the northwest, and (d) the Niger River catchment (Figure 2).

3. Material and Methods

3.1. Quantification of Offshore Accumulation History

We estimated the post-rift accumulation histories of the three rifted margin basins using the method fully detailed in Rouby et al. (2009) and Guillocheau et al. (2011). Only a simplified description of the method, assumptions and uncertainties assessment approach is provided here, and additional details are given in SI.1.

We constructed 17 geological cross-sections of the rifted-margin basins (Figure 3; Figures S1–S3 in Supporting Information S1) from published geological and seismic sections (e.g., Antobreh et al., 2009; Bennett & Rusk, 2002; Brownfield & Charpentier, 2006; Davison et al., 2016; Delteil et al., 1974; Edwards et al., 1997; Gillard et al., 2017; Kjemperud et al., 1992; Lamarche et al., 1997; Lehner & De Ruiter, 1977; Olyphant et al., 2017; Pautot & Renard, 1973; Sage et al., 1997, 2000; Scarselli et al., 2018; Ye et al., 2019) complemented by some proprietary seismic sections provided by TotalEnergies (one per geological section). We constructed seven cross-sections for the Sierra Leone-Liberia Basin, six for the Ivory Coast-Ghana Basin, and four for the Togo-Benin Basin (Figures 2 and 3; Figures S1–S3 in Supporting Information S1). They include the major post-rift stratigraphic horizons above the break-up unconformity but not the syn-rift accumulation because of its poor imaging on available data.

We calibrated the age of stratigraphic horizons using published biostratigraphic data (e.g., Antobreh et al., 2009; Bennett & Rusk, 2002; Pletsch et al., 2001; Wagner, 2002; Wagner & Pletsch, 2001), as well as proprietary wells provided by TotalEnergies. Due to the uneven availability of biostratigraphic data, we calibrated the age of six horizons in the Sierra Leone-Liberia Basin, 11 in the Ivory Coast-Ghana Basin, and nine in the Togo-Benin Basin (Figure 3, Figures S1–S3 and Table S1 in Supporting Information S1; see Text S1.5 in Supporting Information S1). This defined different time increments of accumulation rate measurements, ranging from 66 Myr (i.e., the entire Cenozoic) in the Sierra Leone-Liberia Basin to 3 Myr (i.e., in the Early Oligocene) in the Ivory Coast-Ghana Basin.

The published and proprietary geological and seismic sections cover only the proximal part of the rifted margin (Figures 2 and 3). Therefore, to encompass the whole post-rift sedimentary wedges, we extrapolated the geological cross-sections landward and oceanward. To do this, we used vintage seismic lines (Delteil et al., 1974; Emery et al., 1975), basement isobath maps (Laske & Masters, 1997) and the ages of oceanic crust (Milesi et al., 2010) (Figures 2 and 3; Figures S1 and S2 in Supporting Information S1). The age of the oceanic crust indeed prescribes the maximum age of sediments deposited on it and drastically reduces the range of possible extrapolations. Nonetheless, within these constraints, we also established several extrapolation hypotheses (usually 3) for

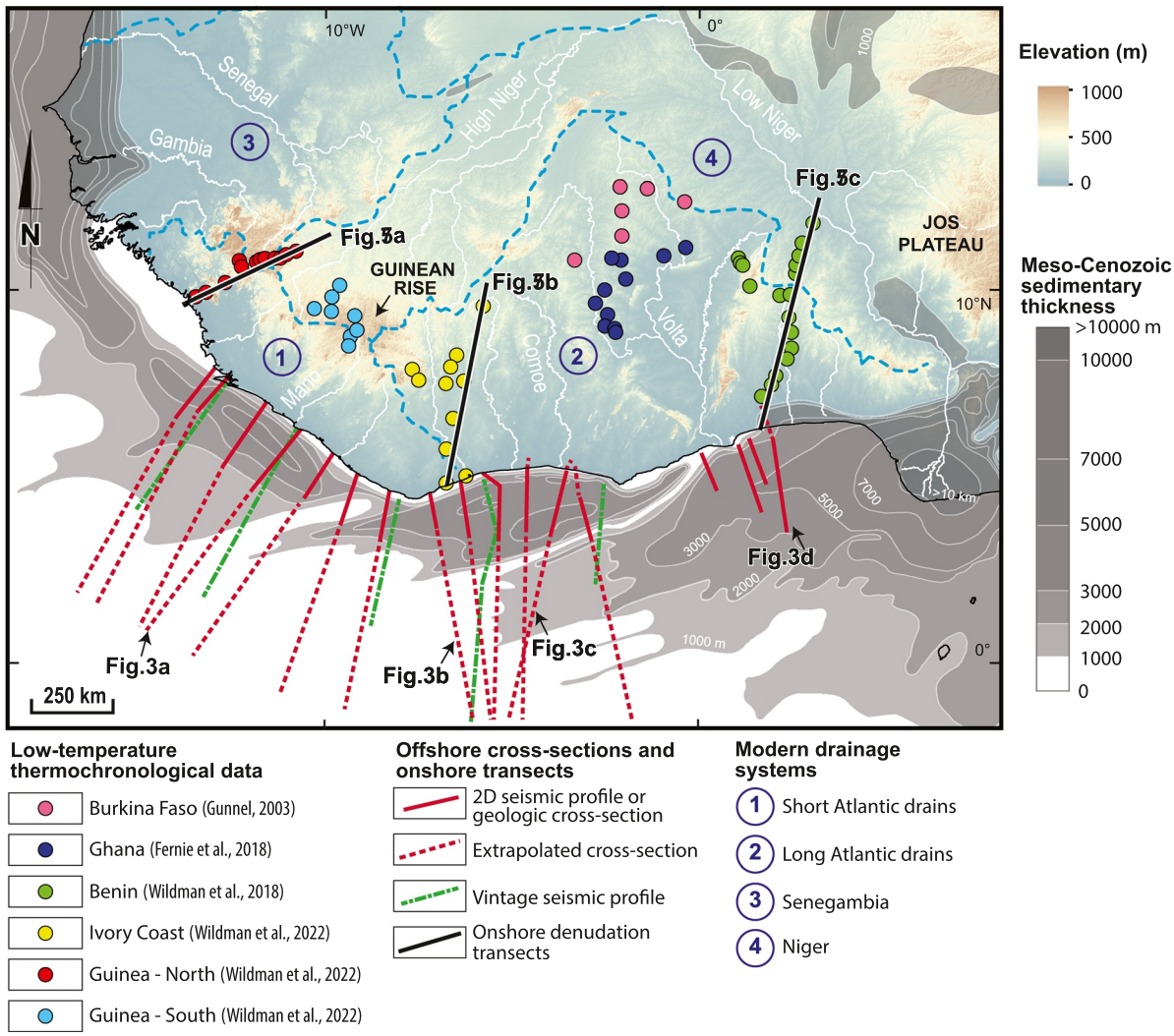

Figure 2. Location map of the data sets. The offshore data set comprises published geological cross-sections and 2D industrial seismic lines (red lines), vintage seismic lines of Emery et al. (1975; in dashed green) and Mesozoic-Cenozoic isopachs after Milesi et al. (2010) (gray contours; thickness values in meters). The extrapolated portions of the 2D industrial cross-sections are shown as red dashed lines and the ones shown in Figure 3 are labeled. The onshore data set comprises the published low-temperature thermochronological samples (colored circles, see Wildman et al. (2022) and references therein). The location of the three denudation transects shown in Figure 5 is indicated by thick black lines. Present day main rivers (white lines) and catchment divides (blue dashed lines) are also displayed. Onshore topography is extracted from Shuttle Radar Topography Mission (SRTM) data set.

each geological cross-section that are included in the estimation of uncertainties (see below). We also used published geological maps (Choubert & Faure-Muret, 1988) to extrapolate the geological cross-sections landward to include the embayment of the Ivory Coast-Ghana and Togo-Benin basins (Figure 2). Note that we did not extrapolate the geological cross-sections in the Togo-Benin Basin oceanward, as the distal part of the basin has received significant lateral supply from the East, probably since the Santonian (~85 Ma; Figure 3d; Figure S3 in Supporting Information S1). Indeed, the Santonian inversion of the Benue Trough generated a mountain range accommodating ~12 km of shortening whose erosion supplied siliciclastic sediments to the surrounding basins (Benkhelil, 1989). The Niger Delta also contributed a large volume of sediments since at least the latest Eocene (Grimaud et al., 2018; Reijers, 2011). We then depth-converted horizons using depth-velocity laws calibrated from proprietary well data (see Text S1.2 in Supporting Information S1). We included uncertainties in these velocities (increasing from 10% to 30% with depth) and incorporated their influence on the estimation of accumulated volumes.

We quantified the volume of sediments accumulated during each time interval in each basin by linear interpolation between the cross-sections (see details in Guillocheau et al. (2011); Figure S6 in Supporting Information S1). To

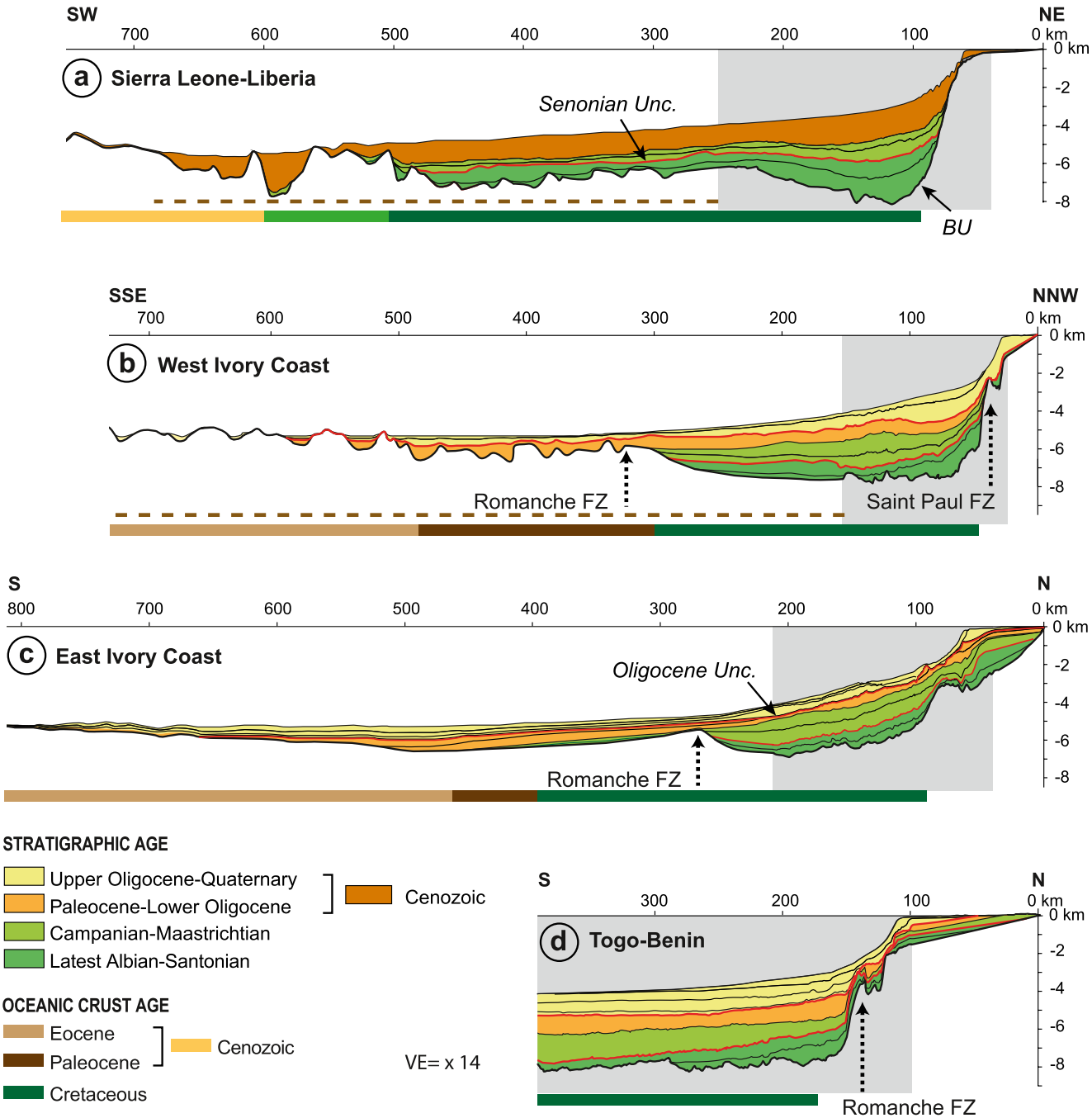

Figure 3. Examples of regional cross-sections built for the estimation of sediment accumulation history in the Sierra Leone-Liberia (a), Ivory Coast-Ghana (b and c) and Togo-Benin (d) basins (see locations on Figure 2). Areas of the cross-sections covered by published and proprietary 2D seismic lines are shown by gray shading and those covered by vintage data by brown dotted lines. Major unconformities are highlighted in red. Ages of oceanic crust are from Milesi et al. (2010). FZ: Fracture Zone. Note that the Togo-Benin geological section is not extrapolated oceanward (see text for details).

extract the siliciclastic solid volumes, we corrected these raw volumes for remaining porosity and in situ carbonate production calibrated from published and proprietary well-data (Antobreh et al., 2009; Bennett & Rusk, 2002; Gonçalves & Ewert, 1998; Pletsch et al., 2001; Strand, 1998; Wagner, 2002; Wagner & Pletsch, 2001) (Figure S4 in Supporting Information S1; see Texts S1.3 and S1.4 in Supporting Information S1). Other in situ productions, such as volcanics, cherts and organic matter, were included in the carbonate content correction, as they have only been very locally observed (e.g., Antobreh et al., 2009; Bennett & Rusk, 2002; Gonçalves & Ewert, 1998; Pletsch et al., 2001; Strand, 1998; Wagner, 2002; Wagner & Pletsch, 2001).

Table 1
Estimated Accumulation Volumes and Rates (and Associated Uncertainties) for Each Time Interval of Each Studied Basin

Basin	Stratigraphic age	Interval (Ma)	Solid volume (10^4 km^3)			Accumulation rate (10^3 km^3/Myr)		
Sierra Leone-Liberia	Cenozoic	66–0	35.4	±	7.4	5.4	±	1.1
	Maastrichtian	72–66	12.0	±	3.5	20.1	±	5.8
	Campanian	85–72	9.2	±	2.0	7.1	±	1.6
	Turonian-Santonian	94–85	8.3	±	1.9	9.3	±	2.1
	Latest Albian-Cenomanian	104–94	7.4	±	1.9	7.4	±	1.9
	TOTAL		**72.5**	**±**	**16.6**	**7.0**	**±**	**1.6**
Ivory Coast-Ghana	Plio-Quaternary	5.3–0	6.6	±	1.1	12.3	±	2.1
	Middle-Upper Miocene	16–5.3	6.2	±	1.3	5.8	±	1.2
	Upper Oligocene-Lower Miocene	31–16	6.9	±	1.5	4.6	±	1.0
	Lower Oligocene	34–31	5.5	±	3.6	18.3	±	12.0
	Eocene	56–34	7.0	±	1.4	3.2	±	0.6
	Paleocene	66–56	6.9	±	1.7	6.9	±	1.7
	Maastrichtian	72–66	8.0	±	2.0	13.3	±	3.3
	Campanian	85–72	8.7	±	1.7	6.7	±	1.3
	Turonian-Santonian	94–85	6.1	±	1.3	6.8	±	1.4
	Latest Albian-Cenomanian	104–94	4.3	±	1.3	4.3	±	2.1
	TOTAL		**66.2**	**±**	**16.8**	**6.4**	**±**	**1.6**
Togo-Benin	Plio-Quaternary	5.3–0	1.1	±	0.1	2.1	±	0.2
	Upper Miocene	11.6–5.3	3.5	±	0.5	5.6	±	0.7
	Middle Miocene	16–11.6	2.2	±	0.4	4.9	±	0.9
	Upper Oligocene-Lower Miocene	31–16	1.0	±	0.2	0.7	±	0.1
	Paleogene	66–31	3.4	±	0.8	1.0	±	0.2
	Campanian-Maastrichtian	85–66	5.1	±	1.0	2.7	±	0.5
	Turonian-Santonian	94–85	2.2	±	0.5	2.4	±	0.6
	Latest Albian-Cenomanian	104–94	3.5	±	1.1	3.5	±	1.1
	TOTAL		**21.9**	**±**	**4.5**	**2.1**	**±**	**0.4**

Note. Bold values are total accumulation values per basin.

Finally, we estimated the uncertainties on solid siliciclastic volumes (km^3) and accumulation rates (km^3/Myr). We used a Monte Carlo simulation combining uncertainties corresponding to each step of the calculation described above (see Guillocheau et al. (2011) for details). This includes (a) the uncertainties in the stratigraphic ages used for calibration of stratigraphic horizons in absolute ages (ranging from 0.5 to 2 Ma; see Table S1 in Supporting Information S1), (b) the uncertainties in the velocity values used for the conversion of the time horizons to depth horizons, (c) uncertainties in the content values used for the in situ production correction (±100% in in-situ content; see Figure S4 in Supporting Information S1) and (d) uncertainties related to the various extrapolation hypotheses. The estimated accumulated volumes, accumulation rates and associated uncertainties are shown in Table 1 and Figure 4.

Sadler (1999) has shown that longer intervals likely incorporate more and longer sedimentation hiatuses (unconformities in particular) than shorter intervals, resulting in lower accumulation rates. To evaluate this time-span effect, we checked the relationship between time interval durations. As accumulation rates indeed tend to be higher for shorter time intervals (Figures S5a–S5c in Supporting Information S1), we also calculated accumulation rates over five even time steps (20.8 Myr; "resampled" rates; Table S2 and Figures S5d–S5f in Supporting Information S1).

3.2. Estimation of Onshore Denudation

To estimate the onshore denudation history, we compiled the published modeled thermal histories of Low-Temperature Thermochronological data (LTT; apatite fission tracks and apatite (U-Th-Sm)/He) of onshore

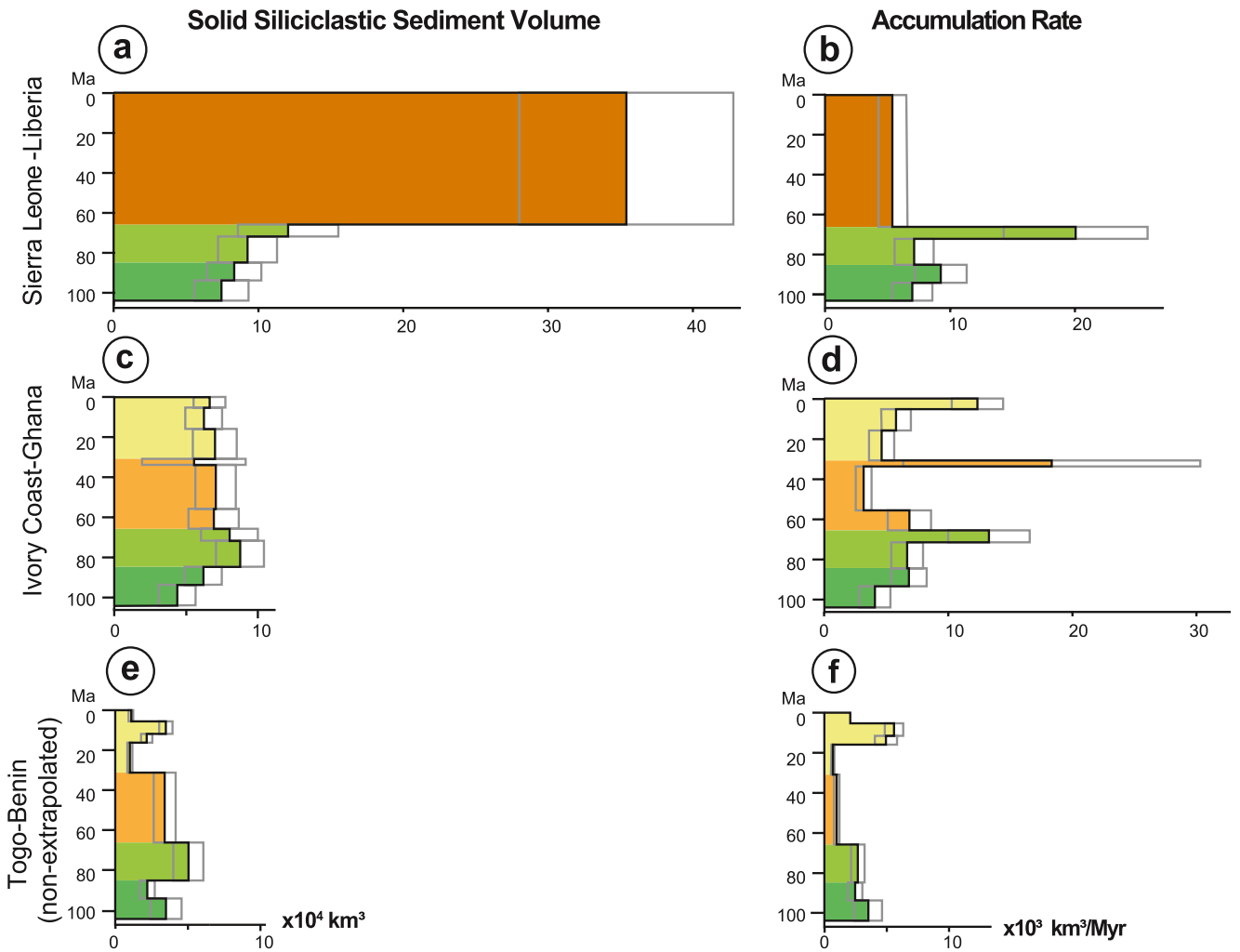

Figure 4. Accumulated volumes and accumulation rates estimated from extrapolated cross-sections in the Sierra Leone-Liberia (a and b) and Ivory Coast-Ghana basins (c and d), and from non-extrapolated cross-sections in the Togo-Benin basin (e and f). Associated uncertainties are shown by gray lines (see text and Table 1 for details).

samples (Figure 2; Figures S6 and S7 and Tables S3 and S4 in Supporting Information S1). We use the study of Gunnell (2003) in Burkina Faso, Fernie et al. (2018) in Ghana, Wildman et al. (2018) in Benin, and Wildman et al. (2022) in Ivory Coast and Guinea. We assumed that, during the modeled period, cooling or heating of samples was primarily driven by unroofing or burial. We also assumed that the output of the various modeling techniques in the published thermal histories is comparable. Following the method of Wildman et al. (2018), we used the preferred thermal model of the original authors to estimate the unroofing/burial history of each sample and the 95% credible intervals (interval including 95% of the probable paths) to estimate the associated uncertainties. We used Equation 1:

$$d = (T_1 - T_2) / (G\,(t_1 - t_2)), \quad (1)$$

where d is the denudation/burial rate (km/Myr), T_1 and T_2 are the temperatures (°C) at time t_1 and time t_2 (Ma), and G is the geothermal gradient (°C/km). Following the method of Wildman et al. (2018), we used an average paleo-geothermal gradient of 25°C/km, which is a typical geothermal gradient for the first 3–5 km of continental crust in cratonic domains (Dipietro, 2013). Wildman et al. (2022) estimated uncertainties associated with paleo-geothermal gradients ranging from 20 to 70°C/km on these denudation estimations. Denudation histories and associated uncertainties of all samples are given in Tables 2 and 3.

Following the method of Wildman et al. (2018), we visualize the denudation/burial history of each margin segment along three transects, perpendicular to the margin segments in Guinea, Ivory Coast and Benin. To do

Table 2
Estimated Denudation and Denudation Rates for the Transect Samples per Time Interval (135–120 Ma, 120–100 Ma, 100–85 Ma, 85–65 Ma, 65–30 Ma, and 30–0 Ma)

			Denudation (m)							Denudation rate (m/Ma)					
Sample	Long	Lat	0–30	30–65	65–85	85–100	100–120	120–135	Total	0–30	30–65	65–85	85–100	100–120	120–135
Guinea Transect: Wildman et al. (2022)															
GN1	−13.42	9.73	400	−520	80	840	1,480	400	3,200	13	−15	4	56	74	27
GM1	−13.42	9.72	400	−520	80	840	1,480	400	3,200	13	−15	4	56	74	27
GM2	−13.37	9.72	400	−520	80	840	1,480	400	3,200	13	−15	4	56	74	27
GN4	−13.14	9.83	400	−520	80	840	1,480	400	3,200	13	−15	4	56	74	27
GM3	−13.14	9.83	400	−520	80	840	1,480	400	3,200	13	−15	4	56	74	27
GN6	−12.63	10.10	120	120	80	80	560	40	1,000	4	3	4	5	28	3
GN7	−12.27	10.69	120	120	80	80	560	40	1,000	4	3	4	5	28	3
GN8	−12.19	10.51	120	120	80	80	560	40	1,000	4	3	4	5	28	3
GN9	−11.81	10.66	200	80	40	80	320	480	1,200	7	2	2	5	16	32
GN10	−11.71	10.70	200	80	40	80	320	480	1,200	7	2	2	5	16	32
GM12	−11.58	10.73	200	80	40	80	320	480	1,200	7	2	2	5	16	32
GM13	−11.29	10.74	200	240	120	120	360	480	1,520	7	7	6	8	18	32
GN11	−11.16	10.73	280	120	120	160	440	320	1,440	9	3	6	11	22	21
GM14	−11.00	10.82	280	120	120	160	440	320	1,440	9	3	6	11	22	21
GN12	−10.75	10.92	280	120	120	160	440	320	1,440	9	3	6	11	22	21
Ivory Coast Transect: Wildman et al. (2022)															
SA-3		−6.63		−80	4.73	80	920	440	3,000	15	−2	0	5	0	104
SA-14		−6.11		−80	4.93	80	920	440	3,000	15	−2	0	5	0	104
SOK1A	−6.65	5.68	320	240	80	120	600	40	1,400	11	7	4	8	30	3
DLO3bisA	−6.46	6.50	320	80	240	120	600	40	1,400	11	7	4	8	30	3
VAAL-1	−6.64	7.41	360	200	120	120	520	480	1,800	12	6	6	8	26	32
BEZ-1	−6.16	7.46	360	200	120	120	520	480	1,800	12	6	6	8	26	32
SEN1	−6.53	7.83	240	80	0	40	80	0	440	8	2	0	3	4	0
MK64	−6.36	8.16	240	80	0	40	80	0	440	8	2	0	3	4	0
KG33	−5.65	9.47	240	200	80	40	120	120	800	8	6	4	3	6	8
Benin Transect: Wildman et al. (2018)															
BN18	1.82	7.06	280	280	160	720	800	80	2,320	9	8	8	48	40	5
BN1	2.09	7.40	1,080	−840	280	600	440	400	2,800	36	−24	14	40	22	27
BN2	2.19	7.62	520	360	−80	−40	80	440	1,400	17	10	−4	−3	4	29
BN3	2.50	8.05	440	240	80	0	880	2,120	3,760	15	7	4	0	44	141
BN17	2.63	8.36	1,040	560	−280	40	1,560	1,040	4,240	35	16	−14	3	78	69
BN4	2.61	8.75	480	−120	160	680	1,480	680	3,360	16	−3	8	45	74	45
BN5	2.55	9.19	680	−400	−240	80	1,120	1,920	3,800	23	−11	−12	5	56	128
BN12	2.30	9.77	360	160	0	0	−40	−80	5,200	12	5	0	0	−2	−5
BN11	2.60	9.77	360	360	200	200	200	160	1,480	12	10	10	13	10	11
BN10	2.72	10.37	680	400	40	40	−40	0	1,160	23	11	2	3	−2	0
BN9	2.73	10.59	0	640	600	−320	−800	−80	3,040	0	18	30	−21	−40	−5
BN8	2.81	10.80	0	1,080	280	−480	−480	−80	1,360	0	31	14	−32	−24	−5
BN7	2.90	11.14	0	280	200	−200	−200	120	600	0	8	10	−13	−10	8
BN6	3.19	11.68	0	880	480	−520	−240	800	2,060	0	25	24	−35	−12	53

Note. Negative denudation is burial. Sources are Wildman et al. (2022) for the Guinea and Ivory Coast transects and Wildman et al. (2018) for the Benin transect.

this, we projected perpendicularly the sample locations on the transect and plotted the incremental denudation estimations at each sample projected location along the transect (Figures 2 and 5; Table 2).

Finally, we estimated the volumes eroded in the area of the margin portion feeding the rifted margin basins for the Guinea and Ivory Coast margin segments (Figure 6). We did not consider the Benin transect in this part of the analysis for two reasons. Firstly, we did not extrapolate the geological cross-sections along the Benin segment because of the lateral sedimentary input (see above). Secondly, the denudation transect shows more complex features than the other two segments, with the potential reactivation of Precambrian shear zones suggested by Fernie et al. (2018) (see details in results section and Wildman et al. (2018)). As the studied area is located within an anorogenic domain, we estimated the denudated volumes assuming that the denudation rates measured along each denudation transect could be generalized to the entire length of the corresponding segment (600 km in length for the Guinea segment and 700 km for the Ivory Coast segment; Figure 6a). We estimated the width of the denudation area feeding the rifted margin basins from the paleogeographic reconstructions of Ye et al. (2017). We used a width of the erosion domain ranging from 100 to 350 km to estimate uncertainties associated with the location of the drainage divide separating sedimentary supply to the intracratonic basin and the rifted margin basins (Figure 6a).

4. Results

4.1. Solid Clastic Sediment Accumulation Histories

4.1.1. Regional Post-Rift Stratigraphic Architectures

The stratigraphic architecture of post-rift sediments varies significantly along the African Equatorial Atlantic rifted margin (Figure 3; Figures S1–S3 in Supporting Information S1). In the Sierra Leone-Liberia Basin, most of post-rift sediments are preserved on the slope and the abyssal plain and only very thin Cenozoic deposits are preserved on the shelf (Figure 3a). In the Ivory Coast-Ghana Basin, the Upper Cretaceous sedimentary wedge is bounded oceanward by the Romanche Fracture Zone, whereas the Cenozoic wedge extends basinward beyond (Figures 3b and 3c). Within this basin, along the eastern divergent rifted margin segment, Upper Cretaceous transitional to shallow-marine sediments are preserved on the shelf (Figure 3c). In contrast, along the western transform segment, Upper Cretaceous sediments by-passed the shelf and are preserved only on the basin slope and floor (Figure 3b) (Ye et al., 2019). In the Togo-Benin Basin, both Upper Cretaceous and Cenozoic deposits are preserved on the shelf (Figure 3d). Oceanward thickening of the sedimentary wedge in the abyssal plain marks the lateral input of sediments from the East (i.e., the Niger Delta) during the Cenozoic (Figure 3d) (Grimaud et al., 2018).

Despite these differences, the post-rift stratigraphic architectures of the three basins share similar regional stratigraphic trends (Figure 3; Figures S1–S3 in Supporting Information S1). Upper Cretaceous sedimentary wedges are generally thicker than Cenozoic wedges. In addition, the extent of Upper Cretaceous sedimentary wedges is limited by major facture zones, whereas Cenozoic wedges are spread over wider unconfined areas. This suggests that fracture zones formed bathymetric barriers for sediment transport during the Late Cretaceous and were then buried in the Cenozoic.

4.1.2. Offshore Accumulation Histories

The Sierra Leone-Liberia Basin recorded a steady increase in accumulated volumes over the Late Cretaceous (from ~7.4 to ~12×10^4 km^3 between 104 and 66 Ma; Figure 4a; Table 1). Accumulation rates remained relatively low during the early post-rift (latest Albian-Campanian; 104–72 Ma; ~7.1 to ~9.3×10^3 km^3/Myr; Figure 4d), increased to the highest value at the end of the Cretaceous (Maastrichtian; 72–66 Ma; ~20.1×10^3 km^3/Myr) and decreased to the lowest in the Cenozoic (66–0 Ma; ~5.4×10^3 km^3/Myr; Figure 4b).

The Ivory Coast-Ghana Basin recorded three highs in accumulation rates (Figure 4d). From low values during the Late Cretaceous (latest Albian-Cenomanian; 104–94 Ma; 14.3—6.8×10^3 km^3/Myr), accumulation rates increased up to the end of the Cretaceous (Maastrichtian; 72-66 Ma; ~13.3×10^3 km^3/Myr). They then decreased to the minimum value in the Eocene (56-34 Ma; ~3.2×10^3 km^3/Myr) and increased again to the maximum value in the Early Oligocene (34-31 Ma; ~18.3×10^3 km^3/Myr). During the Neogene (23-0 Ma), they first decreased (from ~4.6 to ~5.8×10^3 km^3/Myr) before increasing to the final high of the Plio-Pleistocene (~12.3×10^3 km^3/Myr).

In the Togo-Benin Basin, because we used non-extrapolated cross-sections (i.e., without the distal part of the sediment wedge), accumulated volumes and accumulation rates are lower than in the other two basins (Figures 4e and 4f). Accumulation history in the proximal part of the rifted margin recorded three highs, in

Table 3
Estimated Denudation and Denudation Rates per Time Interval (135–120 Ma, 120–100 Ma, 100–85 Ma, 85–65 Ma, 65–30 Ma, and 30–0 Ma) for Samples Not Located on the Transects of Table 2

				Denudation (m)							Denudation rate (m/Ma)					
Loc	Sample	Long	Lat	0–30	30–65	65–85	85–100	100–120	120–135	Total	0–30	30–65	65–85	85–100	100–120	120–135
GU	GN13	−9.53	10.02	440	320	160	200	280	160	1,560	15	9	8	13	14	11
GU	GN16	−9.76	9.71	480	520	360	200	360	160	2,080	16	15	18	13	18	11
GU	GN18	−9.81	9.34	360	280	240	120	200	80	1,280	12	8	12	8	10	5
GU	GN19	−10.23	9.41	600	120	160	120	360	160	1,520	20	3	8	8	18	11
GU	GN31	−9.31	8.40	360	240	280	320	520	360	2,080	12	7	14	21	26	24
GU	GN33	−9.25	8.69	360	240	280	320	520	360	2,080	12	7	14	21	26	24
GU	GN34	−9.10	8.88	440	440	320	200	240	200	1,840	15	13	16	13	12	13
GU	GN36	−9.18	9.21	560	−40	280	200	400	280	1,680	19	−1	14	13	20	19
GU	GN37	−9.17	9.21	560	−40	280	200	400	280	1,680	19	−1	14	13	20	19
IV	YAL	−7.56	7.77	200	160	40	80	200	0	680	7	5	2	5	10	0
IV	YOR	−7.39	7.48	440	480	280	280	440			15	14	14	19	22	0
BE	BN13	1.51	10.01	680	480	80	0	−80	−80	1,240	23	14	4	0	−4	−5
BE	BN14	1.19	10.76	−120	120	200	120	120	160	820	−4	3	10	8	6	11
BE	BN15	1.28	10.61	−120	120	200	120	120	160	820	−4	3	10	8	6	11
BE	BN16	1.32	10.56	−120	120	200	120	120	160	820	−4	3	10	8	6	11
BF	BF1	−1.25	12.62	240	240	120	120	120	120	960	8	7	6	8	6	8
BF	BF2	−1.92	11.35	200	200	120	80	120	80	800	7	6	6	5	6	5
BF	BF3	−1.98	12.68	240	280	160	120	200	120	1,120	8	8	8	8	10	8
BF	BF4	−0.25	12.25	200	200	120	80	120	80	800	7	6	6	5	6	5
BF	BF5	−1.93	12.02	240	200	80	160	120	80	880	8	6	4	11	6	5
BF	BF7	−3.20	10.67	120	120	80	0	120	80	520	4	3	4	0	6	5
GH	155	−2.03	10.67	1,280	−200	−160	40	400	1,400	3,120	43	−6	−8	3	20	93
GH	16	−0.89	10.81	720	360	−80	−120	−160	0	1,080	24	10	−4	−8	−8	0
GH	172	−2.28	10.76	920	400	40	40	200	560	2,160	31	11	2	3	10	37
GH	223	−2.46	9.90	920	−120	0	200	920	1,320	3,360	31	−3	0	13	46	88
GH	252	−2.18	8.88	200	160	80	40	80	80	640	7	5	4	3	4	5
GH	278	−2.70	9.54	1,040	120	80	80	200	240	1,760	35	3	4	5	10	16
GH	369	−2.37	9.23	880	−160	−120	−40	40	160	1,080	29	−5	−6	−3	2	11
GH	43	−2.43	8.93	1,160	680	−120	−120	−200	−40	1,840	39	19	−6	−8	−10	−3
GH	446	−2.16	8.79	320	600	320	160	80	0	1,480	11	17	16	11	4	0
GH	598	−1.90	10.19	1,480	160	−200	−40	40	280	1,960	49	5	−10	−3	2	19
GH	80	−0.28	11.04	880	640	120	0	−80	−120	1,440	29	18	6	0	−4	−8

Note. Negative denudation is burial. Data sources are Wildman et al. (2022) for Guinea (GU) and Ivory Coast (IV); Wildman et al. (2018) for Benin (BE); Gunnell (2003) for Burkina Faso (BF); Fernie et al. (2018) for Ghana (GH).

the latest Albian-Cenomanian (104-94 Ma; ~3.5 × 10^3 km^3/Myr), the Campanian-Maastrichtian (85-66 Ma; ~2.7 × 10^3 km^3/Myr) and the Late Miocene (11.6–5.3 Ma, ~5.6 × 10^3 km^3/Myr) and a low in the Paleocene-Early Miocene (66-16 Ma; ~0.7–1 x10^3 km^3/Myr).

4.1.3. Uncertainties Associated With Accumulation Histories

Uncertainties estimated for accumulation rates range between 0.1 and 12.0 × 10^3 km^3/Myr, that is, they represent generally less than 50% of the average accumulation rate (Figure 4; Table 1). The only exception is the uncertainty

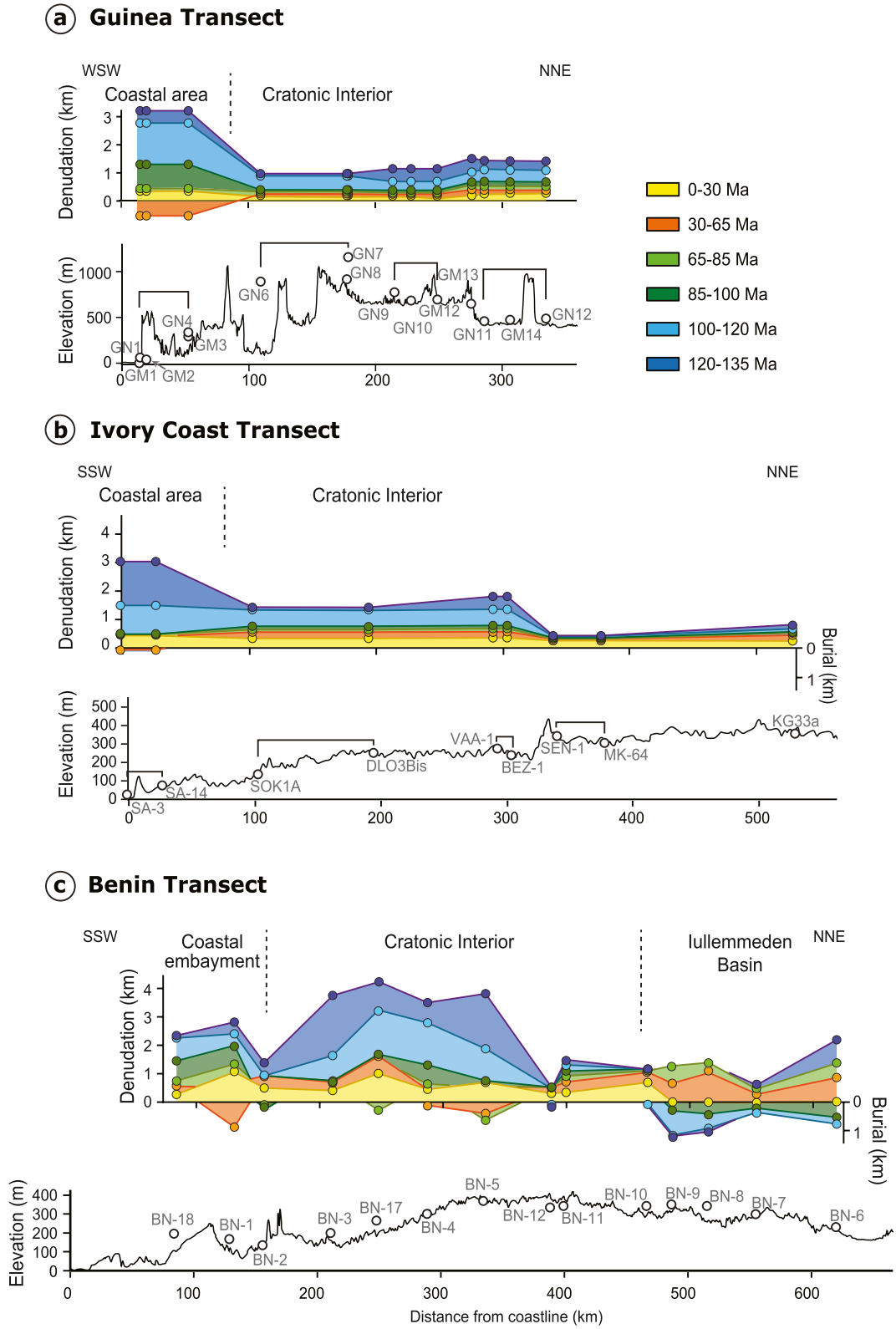

Figure 5. Topographic and incremental denudation transects in (a) Guinea, (b) Ivory Coast and (c) Benin. Sample names are indicated along the topographic profiles above locations shown by circles. The samples modeled together are indicated by square brackets. See location of samples and transects in Figure 2.

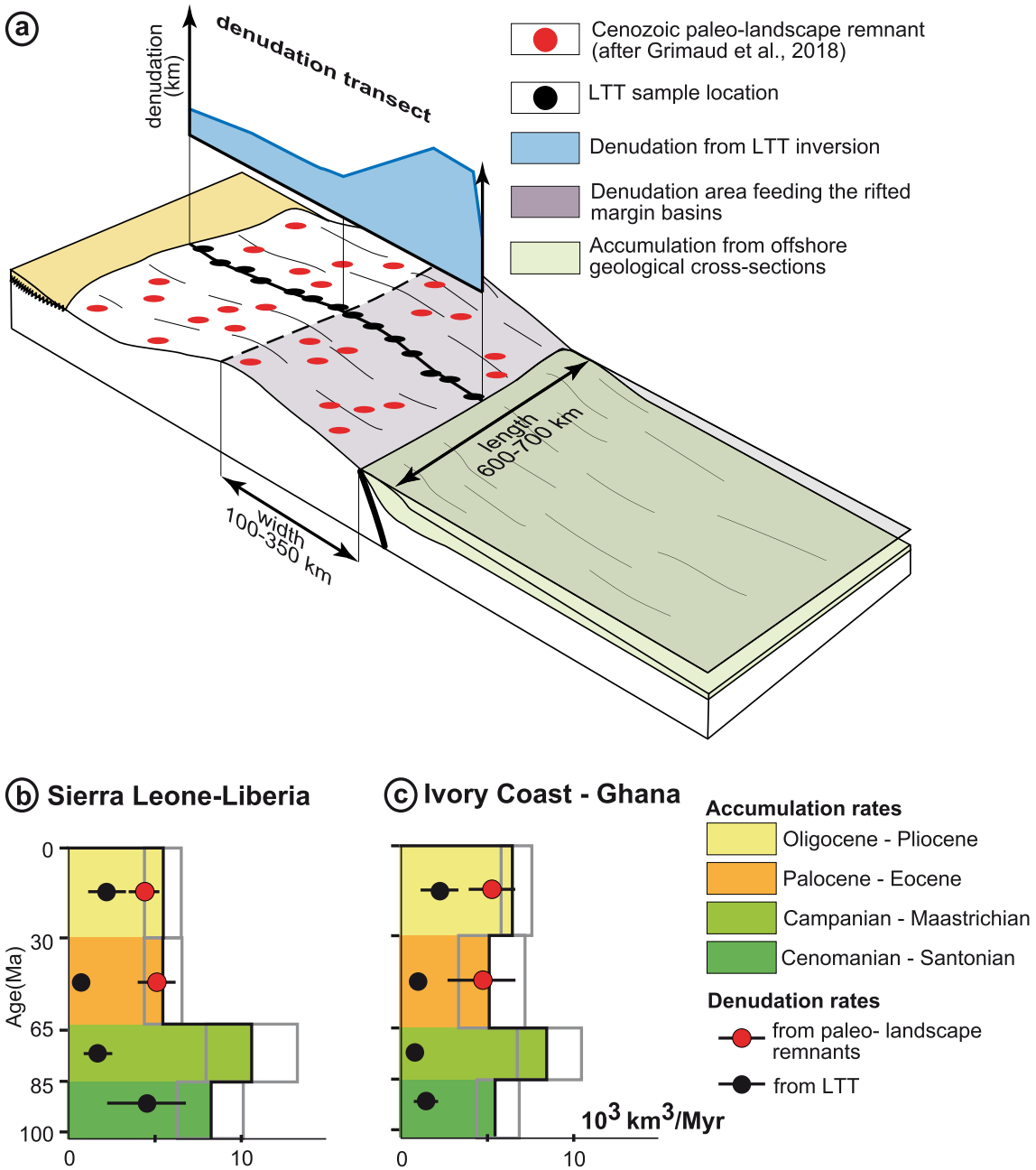

Figure 6. (a) Schematic representation of the approach used to estimate the denudated volumes for each margin segment using (1) the denudation rate measured along the transect (Figures 2 and 5), (2) the length of the margin segment (600 km for Sierra Leone-Liberia; 700 km for Ivory Coast—Ghana) and (3) a width of the coastal area ranging from 100 to 350 km. (b) Denudation/accumulation budget for the Sierra Leone—Liberia Basin and (c) Ivory Coast - Ghana margin segments. Volumetric accumulation rate values are resampled for time increments identical to those of the denudation rates. Volumetric denudation rates and associated uncertainties are estimated from Cenozoic paleo-landform remnants after Grimaud et al. (2018) (red dots with uncertainties) and from LTT data (black dots with uncertainties).

in the accumulation rate estimated between 34 and 31 Ma in the Ivory Coast-Ghana Basin that reaches 65% for a very high accumulation rate (Figure 4d; Table 1).

The resampled accumulation rates allow to include the time span effect (Figure S5 in Supporting Information S1; Sadler (1999)). In the Sierra Leone-Liberia and Ivory Coast-Ghana Basins, the resampled accumulation rates for the Late Cretaceous (104–66 Ma) increase although to lower values than the non-resampled Campanian-Maastrichtian interval (83–62 Ma; Figures S5d and S5e in Supporting Information S1). In the Ivory Coast-Ghana and Togo-Benin Basins, the Paleocene-Eocene low (66–34 Ma) and Middle-Late Miocene high

(ca. 16–5.3 Ma) are preserved in the resampled accumulation rates (Figures S5e and S5f in Supporting Information S1). However, in the Ivory Coast-Ghana Basin, the Early Oligocene (34-31 Ma) high is not reproduced in the resampled accumulation rates (Figure S5e in Supporting Information S1). Overall, even including the uncertainties and the time-span effect, our results firmly establish a general increase in accumulation rates during the Late Cretaceous and low values in the Paleocene-Eocene.

4.2. Onshore Denudation Histories

4.2.1. Denudation Histories

Denudation histories derived from LTT data show different patterns along the rifted margin (Figure 5; Table 2). In Guinea, the coastal and cratonic interior samples show contrasting denudation histories (Figure 5a). The total denudation since 135 Ma is higher (over 3 km) within a narrow coastal area (within 100–200 km from the coast) than in the inland cratonic interior (less than 2 km; Figure 5a). Between 135 and 90 Ma, coastal samples recorded denudation rates of 30–50 m/Myr, while cratonic interior samples recorded decreasing denudation rates from ∼20 to 4–8 m/Myr (Figure 5a). Afterward, all samples recorded slow or negligible denudation rates (<10 m/Myr; Figure 5a).

Similarly, in Ivory Coast, total denudation since 135 Ma is higher (by ∼3 km) within a narrow coastal area than in the cratonic interior (<2 km; Figure 5). Coastal samples recorded high denudation rates (up to 100 m/Myr) during the Early Cretaceous (135–100 Ma), followed by very low denudation rates afterward (∼10 m/Myr; Figure 5b).

In Benin, the denudation transect has 4 segments (see Wildman et al., 2018) (Figure 5c). The northernmost and southernmost segments correspond to the Iullemmeden Basin and the coastal embayment, respectively. The intervening domain may be divided into two segments. The northern one constitutes a <100 km-wide segment of very low overall denudation, fringing the Iullemmeden Basin (i.e., the intracratonic basin fringe). The southern one occupies a 200 km wide strip of high overall denudation in between the coastal embayment and the intracratonic basin fringe (i.e., cratonic domain). The striking feature of the Benin transect is Early Cretaceous (135–100 Ma) high denudation rate (up to 140 m/Myr) compared to the adjoining continental domains. Over that same period, samples were moderately buried in the Iullemmeden Basin. After 100 Ma, denudation rates remained very low across the entire Benin transect (<10 m/Myr). Farther inland, that is, beyond the denudation transects, denudation rates remained very low except very locally in relation to the reactivation of Precambrian shear zones (Fernie et al., 2018).

4.2.2. Uncertainties Associated With Denudation Histories

Uncertainties associated with denudation estimates mainly result from the uncertainties in thermal history models, the lower sensitivity of LTT above the partial annealing/retention zone and the paleo-geothermal gradient used. Uncertainties in thermal history models correspond to the 95% credible intervals (Figure S7 in Supporting Information S1) and result in uncertainties on denudation rates between ±20% for well-constrained thermal events (i.e., rapid cooling) to over ±200% for less constrained events (i.e., slow cooling or cooling above the partial annealing/retention zone). As limited data are available for revealing the changes of the paleo-geothermal gradient through time, actual uncertainties related to the paleo-geothermal gradient are difficult to evaluate. Wildman et al. (2022) estimated uncertainties associated with paleo-geothermal gradients ranging from 20 to 70°C/km on these denudation estimations. They showed that the gradient does not affect the spatial and temporal trends observed along the denudation transect. Nonetheless, it is conceivable that paleo-geothermal gradients might have been higher along the margin than in the cratonic interior, especially during rifting when the continental crust was being thinned and the mantle was concomitantly rising (e.g., Clift et al., 1997). If so, the Early Cretaceous denudation rates may be overestimated near the coast (i.e., in the coastal strip of Guinea and Ivory Coast margin segments and in the Benin embayment; Figure 5). Still, assuming a very high paleo-geothermal gradient of 50°C/km during the Early Cretaceous for these samples would only reduce the estimated denudation rates by a factor of 2. They would remain as high as 50–70 m/Myr for the samples close to the coast in Guinea and Ivory Coast and north of the coastal embayment in Benin, that is, significantly higher than in the cratonic domain. Thus, uncertainties on paleo-geothermal gradient alone does therefore not alter the spatial and temporal trends observed along the denudation transect. In other words, during rifting, high denudation rates were restricted to the coastal

domain in Guinea and Ivory Coast (and north of the coastal embayment in Benin), whilst low denudation rates prevailed over the entire domain afterward.

5. Discussion

5.1. Onshore Denudation Dynamics

During the Equatorial Atlantic rifting (135–104 Ma), we document a pattern of denudation at the scale of sub-saharan West Africa with high denudation rates (up to ∼140 m/Myr) within a narrow strip (100–250 km wide) along the rifted margin, while the remaining part of the cratonic domain underwent slow and monotonic denudation (<10–20 m/Myr; Figure 5). Afterward (104-0 Ma), the whole continental domain underwent slow and monotonic denudation (<10 m/Myr Figure 5).

Thermochronology data of Wildman et al. (2022) show that the only event significantly affecting the thermal structure of the West African lithosphere at a regional scale has been the Equatorial Atlantic rifting and that it has been stable since. The initially faster denudation strip along the rifted margin during the Equatorial Atlantic rifting and immediately after was most probably driven by the erosion of the rift-related relief. Indeed, the width of the higher denudation domain (few hundreds of km) falls within the range expected for flexural rift-shoulder relief produced by crustal thinning (e.g., Buck, 1991; van der Beek et al., 1994). In Benin, the denudation domain is located north of the embayment and is wider than that in Guinea and Ivory Coast. This is probably related to more complex rifting kinematics controlled by structural inheritance (Fernie et al., 2018; Wildman et al., 2018).

After rifting, denudation rates in the high denudation domains dropped to very low cratonic values (∼10 m/Myr; Figures 6d and 6e). This is consistent with rapid relaxation of rift-related relief after break-up as documented along the Central and South Atlantic rifted margins (Rouby et al., 2013). This shows that the steady cratonic regime of very low denudation at the scale of the study area, previously documented after 45 Ma by Beauvais and Chardon (2013), was in fact established earlier, ca. 100 Ma. In other words, both thermal and denudational histories demonstrate that no major regional rock uplift occurred over sub-saharan West Africa during the Cretaceous and the Cenozoic besides the rift-related relief build-up and erosion in the Early Cretaceous.

5.2. Post-Rift Accumulation History

At the scale of the African Equatorial Atlantic rifted margin, our estimation of the post-rift accumulation history shows an increase in accumulation rates during the Late Cretaceous, a decrease during the Paleogene and an increase during the Neogene (Figures 4 and 6). Our data complement existing estimates of post-rift sediment fluxes of the African Atlantic rifted margin basins between the Senegal and the Orange Basins (i.e., Baby et al., 2020; Grimaud et al., 2018; Lodhia et al., 2019; Paul et al., 2014) (Figure 7).

In the Paleocene and Eocene, the whole African Atlantic rifted margin recorded very low accumulation, cooling and denudation rates (Figure 7). This suggests a relief stability (i.e., no significant regional rock uplift) at the scale of the study area at the time. At that time, the resampled accumulation rates and the denudation rates estimated from the paleo-landform remnants by Grimaud et al. (2018) were remarkably consistent (Figures 6b and 6c). We interpret this very low denudation/accumulation regime to be linked to a specific climate favoring weathering and sequestration of terrigenous sediments on the continents. Indeed, during this period, carbonate platforms developed in all the coastal basins (e.g., Bennett & Rusk, 2002; Roberts et al., 2007), as well as wide spread deposition of basic chemical sedimentary associations of chert, flint, phosphate, dolomite, glauconite and montmorillonite, with attapulgite as the dominant clay mineral (Millot, 1970). Very low clastic inputs and correlative chemical sedimentation are primarily linked to extreme chemical weathering that produced extensive thick, lateritic weathering mantles (including bauxites) over most of the continent at the time (Chardon, 2023; Valeton, 1991). Such a cratonic weathering regime, known as biostasy (Erhart, 1956, see Chardon, 2023), was produced by the global greenhouse climate peaking at the Early Eocene climatic optimum (Zachos et al., 2001) and affected the shields of the southern continents (Bardossy & Aleva, 1990; Chardon, 2023; Prasad, 1983). Continental-scale biostasic chemical weathering enhanced production and storage of clastic sediments in thick forest-protected soils and favored solute riverine exports to the ocean and, ultimately, estuarian and marine chemical sedimentation (e.g., Millot, 1970).

10.1029/2023GC010901

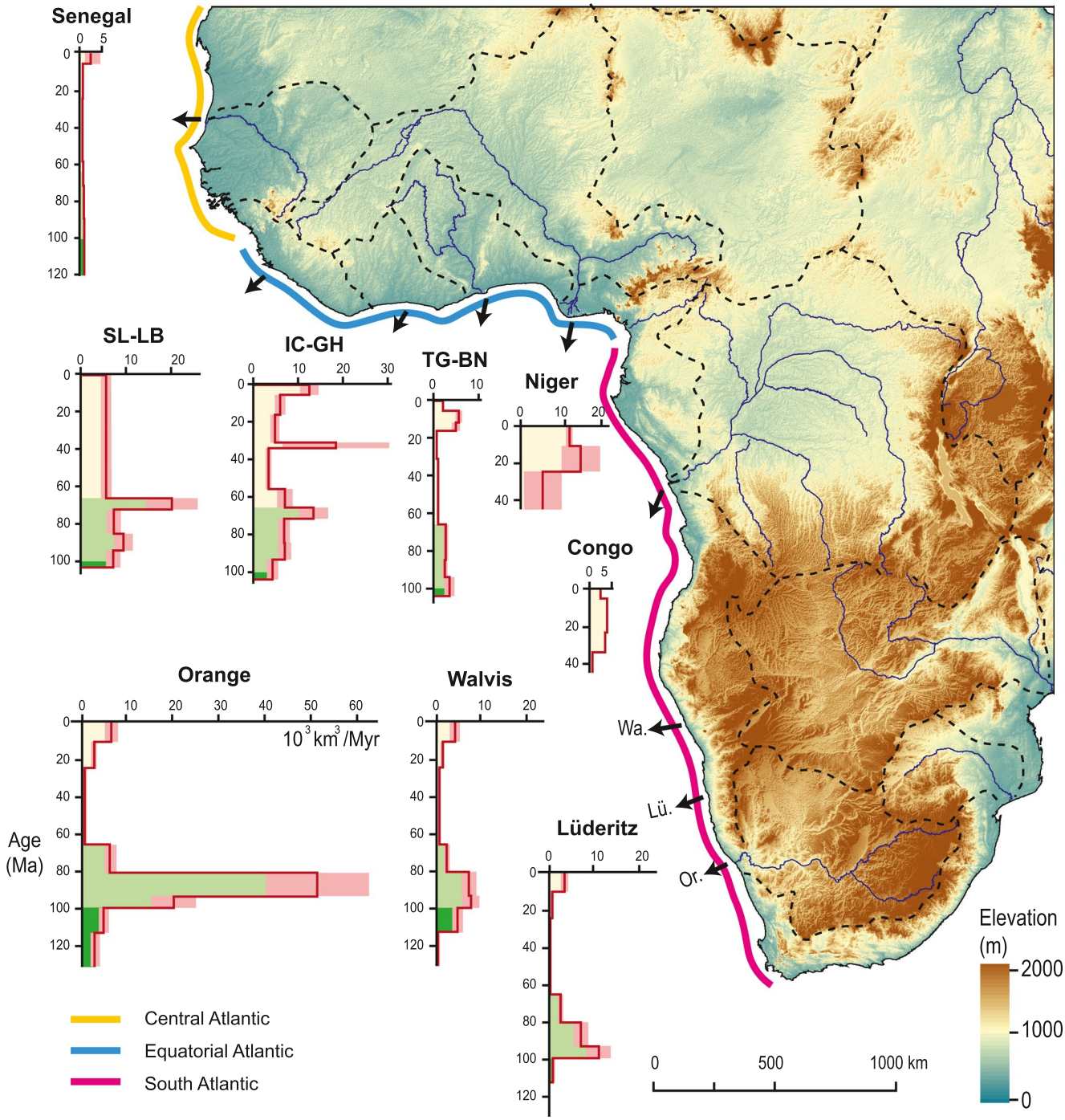

Figure 7. Compilation of solid sediment flux (10^3 km^3/Myr) along the African Atlantic rifted margins. The topographic map of the African continent shows today's main watersheds (black dashed lines) and rivers (blue lines). Solid sediment fluxes of the Sierra Leone-Liberia (SL-LB), Ivory Coast-Ghana (IC-GH) and Togo-Benin (TG-BN) basins are from this study. Fluxes for Senegal from Lodhia et al. (2019), Niger from Grimaud et al. (2018), and Congo from Paul et al. (2014). Fluxes for Walvis (Wa.), Lüderitz (Lü.) and Orange (Or.) are from Baby et al. (2020).

Dryer climates and increased climate seasonality accompanying long-term global cooling after the Eocene (e.g., Clift, 2010), as well epeirogeny due to asthenosphere dynamics below Africa (Burke et al., 2003) contributed to reactivating clastic sedimentary fluxes around the continent (e.g., Baby et al., 2020; Grimaud et al., 2018) (Figures 4, 6, and 7). During that post-Eocene period, the resampled accumulation rates and the denudation rates

estimated from the paleo-landscape remnants by Grimaud et al. (2018) are still remarkably consistent (Figures 6b and 6c).

In contrast, in the Late Cretaceous, West and South African Atlantic rifted margin basins show different accumulation histories. In South Atlantic African basins, accumulation rates mark a peak between 80 and 100 Ma (Baby et al., 2020; Guillocheau et al., 2011; Rouby et al., 2009). This peak has been related to the *en masse* uplift of the South African sub-continent, as suggested by contemporaneous high denudation rates recorded by low-temperature thermochronological data (Baby et al., 2020; Stanley et al., 2015; Wildman et al., 2017). In West African Equatorial Atlantic basins, we also document a Late Cretaceous increase in accumulation rates but with a peak toward the end of the Cretaceous (72—66 Ma i.e., Maastrichian; Figures 4 and 6). Thermal and denudation histories show that West Africa did not undergo significant regional uplift after Equatorial Atlantic rifting (ca. 104 Ma. Figure 5). Prolonged stability of the cratonic hinterland is corroborated by the extremely low accumulation rates in the Central Atlantic Senegal basin in the late Cretaceous (Lodhia et al., 2019; Sahabi et al., 2004) (Figure 7). Over the same period, the volume produced by denudation of the continental domain along the Guinea and Ivory Coast margin segments, as estimated from LTT data, decreased while the accumulation rates increased (Figures 6b and 6c). This decrease in denudation rate can be related to the long-term Phanerozoic peak in greenhouse climate and eustatic sea level in the Cenomanian-Turonian (e.g., Haq, 2014; Huber et al., 2018). This greenhouse climate must indeed have had a comparable - if not greater - impact on sediment export to the oceans than the early Paleocene-Eocene greenhouse on the sequestration of clastic sediments on land. Therefore, the Late Cretaceous increase in sediment supplies to Equatorial Atlantic basins from West Africa under a generally low erosional regime was not driven by continental uplift like in South Africa or by climate cooling. It had to be driven by the drainage network expansion, that is, by an increase in drainage areas of rivers feeding the sedimentary basins of the rifted margin.

5.3. An Integrative Source-To-Sink Model of the Margin Long-Term Evolution

Our results allow us to establish an integrative source-to-sink model for the Ivory Coast margin segment (Figure 8). During Equatorial Atlantic rifting (135–104 Ma), we have no estimation of the accumulation history. During that period (135–100 Ma), sediment accumulated in fault bounded tilted block depocenters (e.g., Antobreh et al., 2009; Brownfield & Charpentier, 2006). Continental denudation was focused on a denudation strip near the coast in Guinea and Ivory Coast, which we interpret as the erosion of the rift-related relief (Figures 5 and 8a). This relief must have been drained by two types of river systems: (a) short and steep coastal drainages on the ocean side of the rift shoulders, feeding the rifted margin basins (e.g., Gallagher & Brown, 1999; Summerfield, 1991) and (b) wider and gentler drainages on the continent side of the rift shoulders, feeding a large intracratonic basin that is, the Saharan basin of Ye et al. (2017).

During the immediate post-rift period (104–94 Ma), the rift-related relief was still being eroded more actively than the cratonic hinterland (Figures 5 and 8a). Accumulation rates in the Sierra Leone—Liberia and Ivory Coast basins were similar (ca. 8 km^3 10^3/Myr; Figure 7) and sediment accumulation was geographically constrained by major facture zones (Figure 3).

In the Late Cretaceous (94–66 Ma), denudation rates within the coastal strip dropped down to values similar to those of the cratonic interior (Figure 5). This suggests that the rift related reliefs were mostly eroded away at the time and that the relief of the whole cratonic domain remained very stable (Figure 8b). Over the same period, accumulation rates in the Sierra Leone –Liberia and Ivory Coast basins were similar and both increased (Figures 4 and 7). That increase in sediment supply must have been driven by an increase in the area of the coastal drainage basins feeding the rifted margin basins by inlandward retreat of the continental divide. Along with Gallagher and Brown (1999), Gilchrist and Summerfield (1990), and Summerfield (1991), we attribute this retreat to landward erosion sustained by long-term flexural isostasy of the margin that maintained a dual (i.e., inlandward and oceanward) drainage systems long after rifting (Figure 8b). According to this model, the length of the coastal drainages must have therefore increased hinterlandward while their slopes decreased (e.g., Gilchrist & Summerfield, 1990). Over that period, accumulation was still constrained by major facture zones (Figure 3).

In the Paleogene, both the denudation rates of the hinterland and accumulation rates in the rifted margin basins dropped (Figures 5 and 7) because of the stability of cratonic relief and of the development of thick lateritic weathering mantles produced by the peak greenhouse climate (Figure 8c). Offshore, the accumulation was not

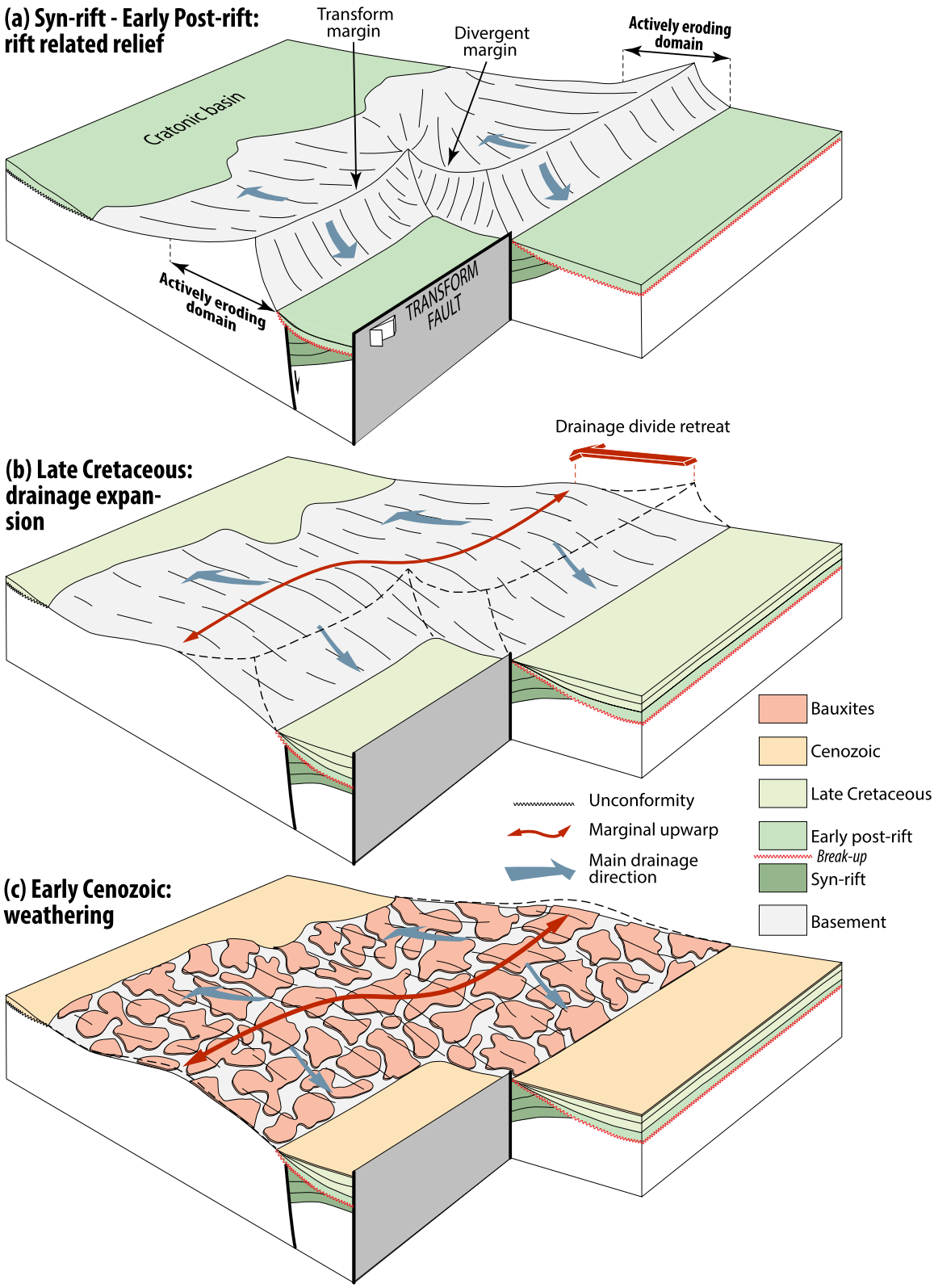

Figure 8. Schematic evolution of the relief and sediment routing systems of the Ivory Coast margin during (a) the syn-rift and early post-rift of the Equatorial Atlantic rift (Early Cretaceous), (b) the Late Cretaceous and (c) Early Cenozoic. Not to scale.

constrained by fracture zones anymore, suggesting that the associated bathymetric barriers subdued in the Cenozoic (Figure 3). Limited Paleocene-Eocene offshore sedimentation was characterized by lithologies typical of biostasy, such as abundant carbonate precipitation and generalized chemical sedimentation.

In the Neogene (<23 Ma) period, denudation rates of the hinterland remained very low (Figure 5) but accumulation rates in the rifted margin basins increased (Figures 4 and 7) (Grimaud et al., 2018). This can be related to the long-term global cooling after the Eocene that favored mechanical erosion. Nevertheless, Chardon et al. (2016) and Grimaud et al. (2018) documented the impact of the growth of the Hoggar hotspot swell on the drainage network organization at the end of the Eocene, resulting in an increase in clastic sediment fluxes.

6. Conclusion

We established the first very long-term (i.e., since 100 Ma) source-to-sink sedimentary budget of sub-saharan West Africa and its Equatorial Atlantic rifted margin using published low-temperature thermochronological data to estimate onshore denudation and regional cross-sections to estimate offshore accumulation.

The major geodynamic event that significantly affected the cratonic source-to-sink regime of the margin was the Equatorial Atlantic rifting. We show that during rifting and immediate post-rift (130–94 Ma), the rise and subsequent erosion of the rift-related relief (i.e., rift shoulders) focused high denudation rates (up to 50–100 m/Myr) along the rifted margin, while the rest of the continental domain underwent steady and very low denudation rates (<10 m/Myr).

After the immediate post-rift, the whole continental domain underwent only very low and steady denudation rates, indicating a stable cratonic relief. Thus, the spatial and temporal variations in accumulation rates in the rifted margin basins were controlled by climate change that modified erosion processes and/or by changes in the size of the drainage areas that modified the sediment routing. In particular, the Late Cretaceous regional increase in accumulation rates was driven by the increase in the drainage areas feeding the basins by a landward migration of the continental divide. By contrast, Paleogene plate-scale decrease in accumulation rates (in the Central, Equatorial and South Atlantic rifted margin basins) was driven by the global greenhouse climate developing thick lateritic weathering mantles storing sediments on the continent and favoring solute riverine exports to the ocean. Neogene resumption of clastic sedimentation responded to both asthenosphere-lithosphere interactions (hot spot swell growth) and mechanical erosion-prone cooler/dryer climates.

Data Availability Statement

All data on sedimentary basins used in this work are published (Antobreh et al., 2009; Bennett & Rusk, 2002; Brownfield & Charpentier, 2006; Davison et al., 2016; Delteil et al., 1974; Edwards et al., 1997; Gillard et al., 2017; Kjemperud et al., 1992; Lamarche et al., 1997; Lehner & De Ruiter, 1977; Olyphant et al., 2017; Pautot & Renard, 1973; Sage et al., 1997, 2000; Scarselli et al., 2018; Ye et al., 2019) except for complementary subsurface data (seismic section and calibration wells) used to calibrate the proximal part of the geological cross-sections that we accessed within the « Transform Source To Sink » collaboration project (TotalEnergies-CNRS) and that are under restrictive proprietary license (TotalEnergies) and thus not open for distribution. Replication data are available in Rouby (2023).

Acknowledgments
This study was funded by TotalEnergies in the framework of the Transform Source-to-Sink Project (TS2P). We acknowledge the TotalEnergies R&D group for providing us with subsurface data, as well as for scientific and technical support. The manuscript benefited from the constructive remarks of R. Charton and 2 anonymous referees.

References

Allen, P. A. (2008). From landscapes into geological history. *Nature*, *451*(7176), 274–276. https://doi.org/10.1038/nature06586

Allen, P. A., Armitage, J. J., Carter, A., Duller, R. A., Michael, N. A., Sinclair, H. D., et al. (2013). The Qs problem: Sediment volumetric balance of proximal foreland basin systems. *Sedimentology*, *60*(1), 102–130. https://doi.org/10.1111/sed.12015

Antobreh, A. A., Faleide, J. I., Tsikalas, F., & Planke, S. (2009). Rift–shear architecture and tectonic development of the Ghana margin deduced from multichannel seismic reflection and potential field data. *Marine and Petroleum Geology*, *26*(3), 345–368. https://doi.org/10.1016/j.marpetgeo.2008.04.005

Baby, G., Guillocheau, F., Braun, J., Robin, C., & Dall'Asta, M. (2020). Solid sedimentation rates history of the Southern African continental margins: Implications for the uplift history of the South African Plateau. *Terra Nova*, *32*(1), 53–65. https://doi.org/10.1111/ter.12435

Bardossy, G., & Aleva, G. J. J. (1990). *Lateritic Bauxites*, developments in economic geology. Elsevier.

Basile, C., Mascle, J., & Guiraud, R. (2005). Phanerozoic geological evolution of the Equatorial Atlantic domain. *Journal of African Earth Sciences*, *43*(1–3), 275–282. https://doi.org/10.1016/j.jafrearsci.2005.07.011

Beauvais, A., & Chardon, D. (2013). Modes, tempo, and spatial variability of Cenozoic cratonic denudation: The West African example. *Geochemistry, Geophysics, Geosystems*, *14*(5), 1590–1608. https://doi.org/10.1002/ggge.20093

Benkhelil, J. (1989). The origin and evolution of the cretaceous Benue trough (Nigeria). *Journal of African Earth Sciences*, *8*(2–4), 251–282. https://doi.org/10.1016/s0899-5362(89)80028-4

Bennett, K. C., & Rusk, D. (2002). Regional 2D seismic interpretation and exploration potential of offshore deepwater Sierra Leone and Liberia, West Africa. *The Leading Edge*, *21*(11), 1118–1124. https://doi.org/10.1190/1.1523743

Bhattacharya, J. P., Copeland, P., Lawton, T. F., & Holbrook, J. (2016). Estimation of source area, river paleo-discharge, paleoslope, and sediment budgets of linked deep-time depositional systems and implications for hydrocarbon potential. *Earth-Science Reviews*, *153*, 77–110. https://doi.org/10.1016/j.earscirev.2015.10.013

Blarez, E., & Mascle, J. (1988). Shallow structures and evolution of the Ivory-Coast and Ghana transform margin. *Marine and Petroleum Geology*, *5*(1), 54–64. https://doi.org/10.1016/0264-8172(88)90039-6

Brownfield, M. E., & Charpentier, R. R. (2006). *Geology and total petroleum systems of the Gulf of Guinea province of West Africa, 2207-C*. U.S Geological Survey Bulletin.

Buck, W. R. (1991). Modes of continental lithospheric extension. *Journal of Geophysical Research*, *96*(B12), 20161–20178. https://doi.org/10.1029/91jb01485

Burke, K., MacGregor, D. S., & Cameron, N. R. (2003). Africa's petroleum systems: Four tectonic "Aces" in the past 600 million years. *Geological Society of London, Special Publication*, *207*, 21–60.

Chardon, D. (2023). Landform-regolith patterns of northwestern Africa: Deciphering Cenozoic surface dynamics of the tropical cratonic geosystem. *Earth-Science Reviews*, *242*, 104452. https://doi.org/10.1016/j.earscirev.2023.104452

Chardon, D., Grimaud, J. L., Rouby, D., Beauvais, A., & Christophoul, F. (2016). Stabilization of large drainage basins over geological time scales: Cenozoic West Africa, hot spot swell growth, and the Niger River. *Geochemistry, Geophysics, Geosystems*, *17*(3), 1164–1181. https://doi.org/10.1002/2015gc006169

Charton, R., Bertotti, G., Duval Arnould, A., Storms, J. E. A., & Redfern, J. (2020). Low-temperature thermochronology as a control on vertical movements for semi-quantitative source-to-sink analysis: A case study for the Permian to Neogene of Morocco and surroundings. *Basin Research*, *12517*(2), 1337–1383. https://doi.org/10.1111/bre.12517

Choubert, G., & Faure-Muret, A. (1988). International geological map of Africa (third edition, scale 1:5,000,000), Paris: Commission for the geological map of the world (CCGM)/UNESCO.

Clift, P. D. (2010). Enhanced global continental erosion and exhumation driven by Oligo-Miocene climate change. *Geophysical Research Letters*, *37*(9), L09402. https://doi.org/10.1029/2010gl043067

Clift, P. D., Lorenz, J., Carter, A., & Hurford, A. J. (1997). Transform tectonics and thermal rejuvenation on the Cote d'Ivoire Ghana margin, West Africa. *Journal of the Geological Society*, *154*(3), 483–489. https://doi.org/10.1144/gsjgs.154.3.0483

Couëffé, R., & Vecoli, M. (2011). New sedimentological and biostratigraphic data in the Kwahu Group (Meso-to Neo-Proterozoic), southern margin of the Volta Basin, Ghana: Stratigraphic constraints and implications on regional lithostratigraphic correlations. *Precambrian Research*, *189*(1–2), 155–175. https://doi.org/10.1016/j.precamres.2011.05.009

Dars, R. (1957). Sur l'existence du Continental intercalaire au NE de Nara (AOF). *Compte Rendu Sommaire des Séances de la Société Géologique de France*, 1957, 248–249.

Davison, I., Faull, T., Greenhalgh, J., O Beirne, E., & Steel, I. (2016). Transpressional structures and hydrocarbon potential along the Romanche fracture zone: A review. *Geological Society, London, Special Publications*, *431*(1), 235–248. https://doi.org/10.1144/SP431.2

Delteil, J. R., Valery, P., Montadert, C., Fondeur, C., Patriat, P., & Mascle, J. (1974). Continental margin in the northern part of the gulf of Guinea. In C. A. Burk, & C. L. Drake (Eds.), *Geology of continental margins* (pp. 297–311). Springer.

Deynoux, M., Affaton, P., Trompette, R., & Villeneuve, M. (2006). Pan-African tectonic evolution and glacial events registered in Neoproterozoic to Cambrian cratonic and foreland basins of West Africa. *Journal of African Earth Sciences*, *46*(5), 397–426. https://doi.org/10.1016/j.jafrearsci.2006.08.005

Dipietro, J. A. (2013). Keys to the interpretation of geological history. In J. A. Dipietro (Ed.), *Landscape evolution in the United States* (pp. 327–344). Elsevier.

Edwards, R. A., Whitmarsh, R. B., & Scrutton, R. A. (1997). The crustal structure across the transform continental margin off Ghana, eastern equatorial Atlantic. *Journal of Geophysical Research*, *102*(B1), 747–772. https://doi.org/10.1029/96JB02098

Emery, K. O., Uchupi, E., Phillips, J., Bowin, C., & Mascle, J. (1975). Continental margin off western Africa: Angola to Sierra Leone. *American Association of Petroleum Geologists Bulletin*, *59*(12), 2209–2265.

Erhart, H. (1956). *La genèse des sols en tant que phénomène géologique: esquisse d'une théorie géologique et géochimique: biostasie et rhexistasie*. Masson.

Fernie, N., Glorie, S., Jessell, M. W., & Collins, A. S. (2018). Thermochronological insights into reactivation of a continental shear zone in response to Equatorial Atlantic rifting (northern Ghana). *Scientific Reports*, *8*(1), 16619. https://doi.org/10.1038/s41598-018-34769-x

Figueiredo, J. J. P., Zalan, P. V., & Soares, E. F. (2007). Bacia da Foz do Amazonas. *Boletim de Geociencias da Petrobras*, *15*, 299–309.

Gallagher, K., & Brown, R. (1999). Denudation and uplift at passive margins: The record on the Atlantic margin of southern Africa. *Philosophical Transactions of the Royal Society A*, *357*(1753), 835–857. https://doi.org/10.1098/rsta.1999.0354

Gilchrist, A. R., & Summerfield, M. A. (1990). Differential denudation and flexural isostasy in formation of rifted-margin upwarps. *Nature*, *346*(6286), 739–742. https://doi.org/10.1038/346739a0

Gillard, M., Sauter, D., Tugend, J., Tomasi, S., Epin, M.-E., & Manatschal, G. (2017). Birth of an oceanic spreading center at a magma-poor rift system. *Scientific Reports*, *7*(1), 15072. https://doi.org/10.1038/s41598-017-15522-2

Gonçalves, C. A., & Ewert, L. (1998). Development of the Cote D'Ivoire-Ghana transform margin: Evidence from the integration of core and wireline log data. *Geological Society, London, Special Publications*, *136*, 375–389. https://doi.org/10.1144/GSL.SP.1998.136.01.30

Gouyet, S. (1988). Evolution tectono-sédimentaire des marges guyanaise et nord-brésilienne au cours de l'ouverture de l'Atlantique Sud (Doctoral dissertation). Université de Pau et des Pays de l'Adour.

Grimaud, J. L., Rouby, D., Chardon, D., & Beauvais, A. (2018). Cenozoic sediment budget of West Africa and the Niger delta. *Basin Research*, *30*(2), 169–186. https://doi.org/10.1111/bre.12248

Guillocheau, F., Rouby, D., Robin, C., Helm, C., Rolland, N., de Veslud, C. L., & Braun, J. (2011). Quantification and causes of the terrigeneous sediment budget at the scale of a continental margin: A new method applied to the Namibia-South Africa margin. *Basin Research*, *24*(1), 3–30. https://doi.org/10.1111/j.1365-2117.2011.00511.x

Gunnell, Y. (2003). Radiometric ages of laterites and constraints on long-term denudation rates in West Africa. *Geology*, *31*(2), 131–134. https://doi.org/10.1130/0091-7613(2003)031<0131:raolac>2.0.co;2

Haq, B. U. (2014). Cretaceous eustasy revisited. *Global and Planetary Change*, *113*, 44–58. https://doi.org/10.1016/j.gloplacha.2013.12.007

Huber, B. T., MacLeod, K. G., Watkins, D. K., & Coffin, M. F. (2018). The rise and fall of the Cretaceous Hot Greenhouse climate. *Global and Planetary Change*, *167*, 1–23. https://doi.org/10.1016/j.gloplacha.2018.04.004

Kilian, C. (1931). Des principaux complexes continentaux du Sahara. *Comptes Rendus Sommaires des Séances de la Société Géologique de France*, *9*, 109–111.
Kjemperud, A., Agbesinyale, W., Agdestein, T., Gustafsson, C., & Yukler, A. (1992). Tectono-stratigraphic history of the Keta Basin, Ghana with emphasis on late erosional episodes. *Bulletin des Centres de Recherches Exploration-Production Elf-Aquitaine - Memoire*, 13, 55–69.
Kuhlemann, J., Frisch, W., Szekely, B., Dunkl, I., & Kazmer, M. (2002). Post-collisional sediment budget history of the Alps: Tectonic versus climatic control. *International Journal of Earth Sciences*, *91*(5), 818–837. https://doi.org/10.1007/s00531-002-0266-y
Lamarche, G., Basile, C., Mascle, J., & Sage, F. (1997). The Cote d'Ivoire–Ghana transform margin. *Geo-Marine Letters*, *17*(1), 62–69. https://doi.org/10.1007/pl00007209
Laske, G., & Masters, G. (1997). A global digital map of sediment thickness. *EOS Transactions American Geophysical Union*, *78*, F483.
Lefranc, J. P. (1983). Corrélation vers le Nord et description stratigraphique detaillée du continental intercalaire (Mésozoïque continental) de la sebkha de Timimouns, Gourara, Sahara algérien: *Comptes Rendus des Séances de l'Académie des Science*s, Série II (pp. 193–196).
Lefranc, J. P., & Guiraud, R. (1990). The continental intercalaire of northwestern Sahara and its equivalents in the neighbouring regions. *Journal of African Earth Sciences*, *10*(1–2), 27–77. https://doi.org/10.1016/0899-5362(90)90047-I
Lehner, P., & De Ruiter, P. A. C. (1977). Structural history of Atlantic margin of Africa. *American Asssociation Petroleum Geologists Bulletin*, *61*(7), 961–981.
Lodhia, B. H., Roberts, G. G., Fraser, A. J., Jarvis, J., Newton, R., & Cowan, R. J. (2019). Observation and simulation of solid sedimentary flux: Examples from Northwest Africa. *Geochemistry, Geophysics, Geosystems*, *20*(11), 4613–4634. https://doi.org/10.1029/2019gc008262
Maffre, P., Ladant, J.-B., Moquet, J.-S., Carretier, S., Labat, D., & Goddéris, Y. (2018). Mountain ranges, climate and weathering. Do orogens strengthen or weaken the silicate weathering carbon sink? *Earth and Planetary Science Letters*, *493*, 174–185. https://doi.org/10.1016/j.epsl.2018.04.034
Markwick, P. J., Paton, D. A., & Mortimer, E. J. (2021). Mapping the complexity of transform margins. *Geological Society, London, Special Publications*, *524*, 245–277. https://doi.org/10.1144/SP524-2021-82
Milesi, J. P., Frizon de Lamotte, D., De Kock, G., & Toteu, F. (2010). *Tectonic Map of Africa* (scale: 1:10,000,000). Paris: Commission de la carte géologique du monde/commission for the geological map of the world (CCGM/CCGM).
Milliman, J., & Farnsworth, K. (2011). In *River discharge to the coastal ocean: A global synthesis*. Cambridge University Press.
Millot, G. (1970). *Geology of clays*. Springer Verlag.
Olyphant, J. R., Johnson, R. A., & Hughes, A. N. (2017). Evolution of the Southern Guinea Plateau: Implications on Guinea-Demerara Plateau formation using insights from seismic, subsidence, and gravity data. *Tectonophysics*, *717*, 358–371. https://doi.org/10.1016/j.tecto.2017.08.036
Paul, J. D., Roberts, G. G., & White, N. (2014). The African landscape through space and time. *Tectonics*, *33*(6), 898–935. https://doi.org/10.1002/2013tc003479
Pautot, G., & Renard, V. (1973). Morphology, limits, origin, and age of salt layer along South Atlantic African margin. *American Association of Petrleum Geologists Bulletin*, *57*(9), 1658–1671. https://doi.org/10.1306/83D91024-16C7-11D7-8645000102C1865D
Pazzaglia, F. J., & Brandon, M. T. (1996). Macrogeomorphic evolution of the post-Triassic Appalachian mountains determined by deconvolution of the offshore basin sedimentary record. *Basin Research*, *8*(3), 255–278. https://doi.org/10.1046/j.1365-2117.1996.00274.x
Pletsch, T., Erbacher, J., Holbourn, A. E. L., Kuhnt, W., Moullade, M., Oboh-Ikuenobede, F., et al. (2001). Cretaceous separation of Africa and South America: The view from the West African margin (ODP leg 159). *Journal of South American Earth Sciences*, *14*(2), 147–174. https://doi.org/10.1016/s0895-9811(01)00020-7
Poag, C. W., & Sevon, W. D. (1989). A record of Appalachian denudation in postrift Mesozoic and Cenozoic sedimentary deposits of the U.S. Middle Atlantic continental margin. *Geomorphology*, *2*(1–3), 119–157. https://doi.org/10.1016/0169-555x(89)90009-3
Prasad, G. (1983). A review of the early Tertiary bauxite event in South America, Africa and India. *Journal of African Earth Sciences*, *1*(3/4), 305–313. https://doi.org/10.1016/s0731-7247(83)80015-9
Reijers, T. (2011). Stratigraphy and sedimentology of the Niger delta. *Geologos*, *17*(3), 133–162. https://doi.org/10.2478/v10118-011-0008-3
Roberts, D. L., Botha, G. A., Maud, R. R., & Pether, J. (2007). Coastal Cenozoic deposits. In M. Johnson, C. Abhaeusser, & R. Thomas (Eds.), *The geology of South Africa* (pp. 605–628). Geological Society of South Africa/Council for Geoscience.
Rouby, D. (2023). Replication data for: Source-to-sink sedimentary budget of the African equatorial Atlantic rifted margin" V1. [Dataset]. Harvard Dataverse. https://doi.org/10.7910/DVN/H5PO4T
Rouby, D., Bonnet, S., Guillocheau, F., Gallagher, K., Robin, C., Biancotto, F., et al. (2009). Sediment supply to the Orange sedimentary system over the last 150 My: An evaluation from sedimentation/denudation balance. *Marine and Petroleum Geology*, *26*(6), 782–794. https://doi.org/10.1016/j.marpetgeo.2008.08.004
Rouby, D., Braun, J., Robin, C., Dauteuil, O., & Deschamps, F. (2013). Long-term stratigraphic evolution of Atlantic-type passive margins: A numerical approach of interactions between surface processes, flexural isostasy and 3D thermal subsidence. *Tectonophysics*, *604*(1–4), 83–103. https://doi.org/10.1016/j.tecto.2013.02.003
Rust, D. J., & Summerfield, M. A. (1990). Isopach and borehole data as indicators of rifted margin evolution in southwestern Africa. *Marine and Petroleum Geology*, *7*(3), 277–287. https://doi.org/10.1016/0264-8172(90)90005-2
Sadler, P. M. (1999). The influence of hiatuses on sediment accumulation rates. *GeoResearch Forum*, *5*, 15–40.
Sage, F., Basile, C., Mascle, J., Pontoise, B., & Whitmarsh, R. B. (2000). Crustal structure of the continent-ocean transition off the Côte d'Ivoire-Ghana transform margin: Implications for thermal exchanges across the palaeotransform boundary. *Geophysical Journal International*, *143*(3), 662–678. https://doi.org/10.1046/j.1365-246x.2000.00276.x
Sage, F., Pontoise, B., Mascle, J., Basile, C., & Arnould, L. (1997). Crustal structure and ocean–continent transition at marginal ridge: The Côte d'Ivoire–Ghana marginal ridge. *Geo-Marine Letters*, *17*(1), 40–48. https://doi.org/10.1007/pl00007206
Sahabi, M., Aslanian, D., & Oliver, J. L. (2004). Un nouveau point de départ pour l'histoire de l'Atlantique central. *Comptes Rendus Geoscience*, *336*(12), 1041–1052. https://doi.org/10.1016/j.crte.2004.03.017
Scarselli, N., Duval, G., Martin, J., McClay, K., & Toothill, S. (2018). Insights into the early evolution of the Côte d'Ivoire margin (West Africa). *Geological Society, London, Special Publications*, *476*(1), 109–133. https://doi.org/10.1144/SP476.8
Schumm, S. A. (1981). Evolution and response of the fluvial system, sedimentologic implications. *The Society of Economic Paleontologists and Mineralogists, Special Publication*, *31*, 19–29.
Sømme, T. O., Helland-Hansen, W., & Granjeon, D. (2009). Impact of eustatic amplitude variations on shelf morphology, sediment dispersal, and sequence stratigraphic interpretation: Icehouse versus greenhouse systems. *Geology*, *37*(7), 587–590. https://doi.org/10.1130/g25511a.1
Stanley, J. R., Flowers, R. M., & Bell, D. R. (2015). Erosion patterns and mantle sources of topographic change across the southern African Plateau derived from the shallow and deep records of kimberlites. *Geochemistry, Geophysics, Geosystems*, *16*(9), 3235–3256. https://doi.org/10.1002/2015gc005969

Strand, K. (1998). Sedimentary facies and sediment composition changes in response to tectonics of the Côte d'Ivoire-Ghana Transform Margin. In J. Mascle, G. P. Lohmann, & M. Moullade (Eds.), *Proceedings of the Ocean Drilling Program, Scientific Results* (Vol. 159, pp. 113–123). Ocean Drilling Program.

Summerfield, M. A. (1991). Sub-aerial denudation of passive margins: Regional elevation versus local relief models. *Earth and Planetary Science Letters*, *102*(3–4), 460–469. https://doi.org/10.1016/0012-821x(91)90036-h

Tinker, J., de Wit, M., & Brown, R. (2008). Linking source and sink: Evaluating the balance between onshore erosion and offshore sediment accumulation since Gondwana break-up, South Africa. *Tectonophysics*, *455*(1–4), 94–103. https://doi.org/10.1016/j.tecto.2007.11.040

Valeton, I. (1991). Bauxites and associated terrestrial sediments in Nigeria and their position in the bauxite belts of Africa. *Journal of African Earth Sciences*, *12*(1–2), 297–301. https://doi.org/10.1016/0899-5362(91)90078-d

van der Beek, P., Cloetingh, S., & Andriessen, P. (1994). Mechanisms of extensional basin formation and vertical motions at rift flanks: Constraints from tectonic modelling and fission-track thermochronology. *Earth and Planetary Science Letters*, *121*(3–4), 417–433. https://doi.org/10.1016/0012-821x(94)90081-7

Wagner, T. (2002). Late cretaceous to early quaternary organic sedimentation in the eastern equatorial Atlantic. *Palaeogeography, Palaeoclimatology, Palaeoecology*, *179*(1–2), 113–147. https://doi.org/10.1016/S0031-0182(01)00415-1

Wagner, T., & Pletsch, T. (2001). No major thermal event on the mid-Cretaceous Côte d'Ivoire-Ghana Transform Margin. *Terra Nova*, *13*(3), 7–171. https://doi.org/10.1046/j.1365-3121.2001.00333.x

Wildman, M., Brown, R., Persano, C., Beucher, R., Stuart, F. M., Mackintosh, V., et al. (2017). Contrasting Mesozoic evolution across the boundary between on and off craton regions of the South African plateau inferred from apatite fission track and (U-Th-Sm)/He thermochronology. *Journal of Geophysical Research: Solid Earth*, *122*(2), 1517–1547. https://doi.org/10.1002/2016jb013478

Wildman, M., Brown, R., Ye, J., Chardon, D., Rouby, D., Kouamelan, A. N., & Dall'Asta, M. (2022). Contrasting thermal evolution of the West African equatorial and central Atlantic continental margins. *Gondwana Research*, *111*, 249–264. https://doi.org/10.1016/j.gr.2022.08.010

Wildman, M., Webster, D., Brown, R., Chardon, D., Rouby, D., Ye, J., et al. (2018). Long-term evolution of the West African transform margin: Estimates of denudation from Benin using apatite thermochronology. *Journal of the Geological Society*, *176*(1), 97–114. https://doi.org/10.1144/jgs2018-078

Wittmann, H., Malusa, M. G., Resentini, A., Garzanti, E., & Niedermann, S. (2016). The cosmogenic record of mountain erosion transmitted across a foreland basin: Source-to-sink analysis of in situ Be-10, Al-26 and Ne-21 in sediment of the Po river catchment. *Earth and Planetary Science Letters*, *452*, 258–271. https://doi.org/10.1016/j.epsl.2016.07.017

Ye, J., Chardon, D., Rouby, D., Guillocheau, F., Dall'asta, M., Ferry, J. N., & Broucke, O. (2017). Paleogeographic and structural evolution of northwestern Africa and its Atlantic margins since the early Mesozoic. *Geosphere*, *13*(4), 1254–1284. https://doi.org/10.1130/GES01426.1

Ye, J., Rouby, D., Chardon, D., Dall'asta, M., Guillocheau, F., Robin, C., & Ferry, J. N. (2019). Post-rift stratigraphic architectures along the African margin of the equatorial Atlantic: Part I the influence of extension obliquity. *Tectonophysics*, *753*, 49–62. https://doi.org/10.1016/j.tecto.2019.01.003

Zachos, J., Pagani, M., Sloan, L., Thomas, E., & Billups, K. (2001). Trends, rhythms, and aberrations in global climate 65 Ma to present. *Science*, *292*(5517), 686–693. https://doi.org/10.1126/science.1059412

Zattin, M., Pace, D., Andreucci, B., Rossetti, F., & Talarico, F. M. (2014). Cenozoic erosion of the transantarctic mountains: A source-to-sink thermochronological study. *Tectonophysics*, *630*(1), 158–165. https://doi.org/10.1016/j.tecto.2014.05.022

References From the Supporting Information

Jones, S. M., White, N., Faulkner, P., & Bellingham, P. (2004). Animated models of extensional basins and passive margins. *Geochemistry, Geophysics, Geosystems*, *5*(8), Q08009. https://doi.org/10.1029/2003gc000658